https://doi.org/10.5194/egusphere-2026-6489
Preprint. Discussion started: 9 November 2026
© Author(s) 2026. CC BY 4.0 License.

How reactive metals and base cations influence soil organic carbon content and dynamics in temperate French forests.

Florian Mézerette[1], Delphine Derrien[1,2], Zhun Mao[3], Pierre Barré[4], François Baudin[5], Manuel Nicolas[6], Laurent Saint-André[1]

[1]Biogéochimie des Écosystèmes Forestiers, INRAE, Centre de Nancy, 54280 Champenoux, France
[2]SAS, INRAE, Institut Agro, 35000 Rennes, France
[3]Univ Montpellier, AMAP, INRAE, CIRAD, CNRS, IRD, 34000 Montpellier, France
[4]Laboratoire de Géologie, École normale supérieure, CNRS, PSL University, IPSL, 75005 Paris, France
[5]Institut des Sciences de la Terre – Paris (ISTeP), Sorbonne Université, CNRS, CY Univ., 75005 Paris, France
[6]Office National des Forêts, Direction Forêts et Risques Naturels, Département Recherche-Développement-Innovation, Boulevard de Constance, 77300 Fontainebleau, France

Correspondence to: Florian Mézerette (florian.mezerette@inrae.fr)

Abstract. Soil organic carbon (SOC) immobilisation and sequestration have been found to be influenced by a wide range of environmental factors, notably the climate, stand characteristics, and soil properties. Recent research has suggested that some soil properties traditionally regarded as major predictors of SOC stocks (e.g. clay content) may be less influential than those pH–dependent, reactive constituents, including crystalline aluminium (Al) and iron (Fe) oxides, and basic cations. However, these soil properties have rarely been considered for explaining large-scale variation in SOC storage. Here, by taking the advantage of the RENECOFOR network double forest soil inventory at a 15–year interval over the French European territory, we investigate how both SOC storage and its temporal dynamics vary as a function of climate, stand characteristics, and soil properties. Furthermore, we used Rock-Eval® (RE) thermal fractionation to identify descriptors correlated with proxies of SOC biogeochemical stability, in particular the hydrogen index (HI – hydrocarbon proportion of SOC) and T_{50} CO_2 PYR (thermal stability indicator positively correlated to SOC biogeochemical stability). While the effect of the cations only occurred when pH ≥ 5, the metal oxides increased SOC for both pH ≥ 5 and pH < 5 groups. These effects were also identified on the thermal stability of C (T_{50} CO_2 PYR) for the 0–10 and 10–20 cm soil layers. No unequivocal relationship was found between HI and soil properties. When considering reactive soil constituents, clay content played a limited role in explaining variations of SOC and RE metrics. While HI was lower in coniferous forests, there was no other clear effect of climate nor stand characteristics. Regarding the C dynamics, only the 0–10 cm layer showed sufficiently high variations to be confidently analysed. For this layer, the expected variables (e.g. temperature or litter input) did not explain any of the variations of SOC or RE metrics. However, the composition of SOC, through tree species or HI, had an influence on the SOC dynamics, with lower SOC variation the more the carbon was labile. Additionally, the variation of SOC was highly influenced by the dynamics of holorganic layers, with a decrease of SOC content variation with an increase of the change of forest floor stock. Our results highlight the generally stronger role of soil factors than climatic or stand ones in explaining

https://doi.org/10.5194/egusphere-2026-6489
Preprint. Discussion started: 9 November 2026
© Author(s) 2026. CC BY 4.0 License.

large-scale variation in forest SOC storage, largely due to the inclusion of refined soil geochemical properties beyond clay content.

Short summary. Recent research on soil organic carbon pointed out the influence of soil properties which effect may vary given the soil pH: basic cations and reactive metals content. These variables were found to be influential on soil organic carbon, but also on the thermal stability of carbon, reflecting its lability. However, the dynamics of carbon at decadal scale were more likely influenced by its own properties rather than soil and even climate in temperate forest stands.

1. Introduction

Soil is the largest terrestrial carbon (C) pool, being a larger stock than the atmosphere and plant biomass combined (Friedlingstein et al., 2025). Furthermore, forest soils harbour larger C–stock per surface than other biomes (Jobbágy and Jackson, 2000), but soil carbon is susceptible to anthropogenic activities and is vulnerable to decomposition driven by climate change and temperature increase (Karhu et al., 2010; Lugato et al., 2021). Forest soils can either act as a C sink or as a source, therefore reducing or exacerbating greenhouse gas emissions (Baldocchi et al., 2018). Forests exhibit important variations in local conditions and soil properties (Osman, 2013), while being a relatively stable ecosystem on a century-long timescale (Beillouin et al., 2023), making this land use particularly appropriate to identify the factors influencing forest soil organic carbon (SOC). Understanding the drivers of variation in forest SOC storage is essential to improve predictions of the terrestrial biogeochemical cycles and to develop effective forest management strategies to enhance C sequestration under global changes. Despite its importance, the biotic and abiotic drivers of variation in forest SOC storage remain poorly understood, resulting in substantial uncertainty in predictions of forest SOC dynamics (Guidi et al., 2025; Mao et al., 2019).

As in other terrestrial ecosystems, changes in forest SOC are determined by the balance between C input and loss. Below- and above-ground plant residues, alongside other sources of inputs, such as root exudates and hyphae, is a primary source of fresh C input for SOC formation (Dignac et al., 2017; Ouimette et al., 2020). In forests, litter typically refers to dead leaves, branches of different sizes, coarse and fine roots, and other organs (e.g. fruits and barks), which may differ in quantity and quality, such as size, shape, and structural and biochemical traits (Mao et al., 2019). These traits modify the decomposition rate of organic matter (Vávřová et al., 2009; Wang et al., 2022) via the interactions with decomposers communities that depolymerise organic residues (Strickland et al., 2009). Decomposer activity mineralising soil organic matter, leaching of dissolved compounds and soil erosion are responsible for C loss. This leads to a vertical stratification of SOC, with its content decreasing and carbon age increasing with depth (Balesdent et al., 2018; Jobbágy and Jackson, 2000), and this relationship depends on the soil nature (Mathieu et al., 2015). Furthermore, the predictors of SOC stocks vary with depth: SOC located in the surface layers has been found to be more influenced by climatic factors and tree species than SOC in deeper layers (Dawud et al., 2016; Jobbágy and Jackson, 2000), while the effects of soil properties are more prevalent in subsoils (Jobbágy and Jackson, 2000; Reichenbach et al., 2021).

https://doi.org/10.5194/egusphere-2026-6489
Preprint. Discussion started: 9 November 2026
© Author(s) 2026. CC BY 4.0 License.

Air temperature and precipitation are widely used as proxies to represent pedoclimatic conditions, because large scale data on soil temperature and moisture are often limited due to their strong intra annual variability and high cost of data collection and monitoring (Liski et al., 2003; Zhang et al., 2015). Soil properties, including texture, cations content, or pH, play a key role in SOC by modifying the stabilisation processes. Clay content (particles < 2 µm), alone or along silt (> 2 µm and < 200 µm), has been found to drive positively the C content (Hassink, 1997), and is widely used to control C dynamics in predictive models (e.g. CENTURY, Millennial, RothC models – Parton et al., 1987; Abramoff et al., 2018; Coleman et al., 2024). But the clay fraction comprises a large variety of minerals (Kleber et al., 2015), and the interaction of organic matter and mineral phases depends on the nature of the clay minerals and OM Bölscher et al. (2025). Clay-sized minerals are mainly composed of phyllosilicates organised in layers (and possibly other aluminosilicates) and by metal oxides and other oxides at a lesser degree (Ito and Wagai, 2017; Kleber et al., 2021). The scientific community has also recently acknowledged that it is important to go "beyond clay" to predict SOC content (Rasmussen et al., 2018). Indeed, metal cations such as aluminium (Al) and iron (Fe) can protect carbon either in adsorption complexes, coprecipitates, or short-range ordered (SRO) minerals. These above two types of organomineral associations reduce SOC accessibility to microbes and enhance its persistence with time (Lavallee et al., 2020). At the continental scale, von Fromm et al. (2021) showed oxalate-extractable aluminium and iron (Al_o, Fe_o) and exchangeable calcium (Ca_{ex}), along other soil characteristics, are as important as climate to explain soil organic carbon content in sub-Saharan Africa. These relationships between C content and oxalate-extracted metals have also been observed at a more local scale (Kleber et al., 2005). pH regulates these associations by affecting soil solution chemistry (Desie et al., 2021). In acid soils, organic matter is mainly in association with Al and Fe in short-range ordered mineral-organic matter complexes, while in more alkaline soil conditions, organic matter is more associated with phyllosilicate with basic cations (i.e. Ca^{2+} and Mg^{2+}) involved in the bridging of organic matter to mineral surfaces (Kleber et al., 2015; Rasmussen et al., 2018).

Among studies investigating SOC, most in situ experiments focused on the drivers of C–stocks or content, and not on their variation. Some have explored how SOC dynamics are controlled at the decadal to centennial timescale, but they have either focused on land use change (Schiedung et al., 2025), on climate effect without considering soil characteristics (Chen et al., 2023), or made in experimentations (Bramble et al., 2024). These studies have shown that SOC changes at decadal to centennial timescale are mainly linked to the carbon pools with short (a few years to a few decades) mean residence times (Schiedung et al., 2025). Furthermore, stand characteristics and soil properties may influence carbon sequestration – with higher SOC accumulation in coniferous stands in goethite clay type (Bramble et al., 2024). Ten years ago, Jonard et al. (2017) investigated the drivers of SOC stock on the 102 sites of the RENECOFOR monitoring network, which is the French node of the International Co-operative Programme on Forests network (ICP Forests). The RENECOFOR network covers a wide range of soils and of tree species, in which the soil organic carbon has been sampled once up to 1 m and twice at a 15–year interval for three soil depths (0–10, 10–20, and 20–40 cm), alongside other geochemical properties. In their analyses, Jonard et al. (2017) found that no soil property was linked to SOC stock variation using variable selection. The main explaining factors was the age of the stand, which decreased the sequestration rate, and the management practices, uneven-

https://doi.org/10.5194/egusphere-2026-6489
Preprint. Discussion started: 9 November 2026
© Author(s) 2026. CC BY 4.0 License.

aged sites sequestrating more C than even-aged stands. Nevertheless, reactive metals were not explicitly included in their analyses. We argue that these omissions may have limited the identification of key soil drivers, as well as the assessment of their relative importance compared with climate and stand-related drivers, in explaining variation in forest SOC storage. Moreover, forest C storage is susceptible to storm disturbances (Mayer et al., 2023). The inclusion of storm-disturbed RENECOFOR plots in the original analyses may have weakened the statistical diagnoses regarding the relationships between SOC storage and its drivers.

Given recent advances in our understanding of SOC stabilisation in mineral soils, we aimed at reanalysing this substantial dataset, but with a renewed approach: (i) we performed a site selection, removing those which have been disturbed by storms; (ii) we investigated the C–content rather than the stock, considering that bulk density would have blurred some relationships (Yang et al., 2022); (iii) we focused on mineral soil, integrating in our models several properties regulating SOC content and dynamics has recently been highlighted; (iv) we chose an a priori set of explanatory variables, and we expected to identify some effects that would have been masked by other variables. Furthermore, new chemical metrics were described to better characterised SOC, using Rock-Eval® 6 thermal analysis (Barré et al., 2024) which can quantify the proportion of poorly decomposed OM assessed by the ratio of hydrocarbons to TOC (Hydrogen Index – HI) and the thermal stability of SOC assessed by the temperature at which 50 % of the CO_2 has been emitted during the pyrolysis ramp of the Rock-Eval® methodology (T_{50} CO_2 PYR). HI is linked to the degree of decomposition of SOM, with highest values observed in fresh or less decomposed SOM (Saenger et al., 2013), while high values of thermal stability as determined by T_{50} CO_2 PYR are linked to a greater biochemical stability (Cécillon et al., 2021) which may be arise from organomineral bonds (Schulten and Leinweber, 1993). We analysed the values of each of these variables (SOC content, HI, and T_{50} CO_2 PYR) for each layer depth (0–10, 10–20, and 20–40 cm) at the second sampling campaign, and their annual variation in a 15–year interval.

Our overall hypotheses are as follows:

(H1) the soil properties which will mainly explain SOC content are reactive metals for lower pH soils, and basic cations (Ca^{2+} and Mg^{2+}) and clay for higher pH soils;

(H2) the effect of climate and stand characteristics on SOC content are higher in surface layers, with reducing influence with depth. On the contrary, soil properties have a greater effect in deeper layers;

(H3) the amount of poorly decomposed carbon, using HI as proxy, is mainly impacted by climate and forest variables (such as mean annual temperature, functional group of the main tree species, etc.), while the more stable C, represented by higher T_{50} CO_2 PYR values, is more dependent on soil properties (such as clay content, reactive metals, etc.);

(H4) the decadal changes in SOC content, HI and T_{50} CO_2 PYR over a decade are less affected by soil properties and mainly regulated by stands characteristics and climate.

https://doi.org/10.5194/egusphere-2026-6489
Preprint. Discussion started: 9 November 2026
© Author(s) 2026. CC BY 4.0 License.

2. Material and Methods

2.1 RENECOFOR dataset and site selection

This monitoring network consists of 102 forest stands distributed across European France and belongs to ICP-Forest European network (Ulrich, 1995). The stands were representative of the country variability in terms of soil type (mainly Cambisol, Luvisol, and Podzol – IUSS Working Group WRB, 2022) and tree species, with seven coniferous species: silver fir (*Abies alba* Mill.), European larch (*Larix decidua* Mill.), Norway spruce (*Picea abies* (L.) H.Karst.), Corsican pine (*Pinus nigra* Arn. subsp. *laricio* (Poir.) Maire var. *corsicana* (Loudon) Hyl.), maritime pine (*Pinus pinaster* Aiton), Scots pine (*Pinus sylvestris* L.), Douglas fir (*Pseudotsuga menziesii* (Mirb.) Franco), and three broadleaf species: European beech (*Fagus sylvatica* L.), sessile oak (*Quercus petraea* (Matt.) Liebl.), and European oak (*Quercus robur* L.). Most stands were in a mature state at the beginning of the monitoring, in the early 1990s, and sustained typical forestry management in France, mainly regular thinning. 5,000 m^2 of the stands was isolated by a fence, where the soil sampling was carried out during two campaigns: in 1993–1995, and in 2007–2012, with an average time span of 16.3 years, and around the same period of the year for a given site.

Eighty sites were selected from the RENECOFOR network (Figure 1), as we excluded stands which were highly disturbed before or during the monitoring period. Natural disturbances might greatly impact the SOC stock, notably after windthrow (Mayer et al., 2023), and consequently, change the usual C dynamics. Therefore, we chose to exclude the stands which sustained more than 50 % reduction in basal area between two inventories, either from natural disturbance or logging, representing 13 stands. We also removed sites whose soil had been perturbed prior to the monitoring, those with incomplete soil analyses, and those with high vegetation differences between the inside and outside of the fence, indicating high ungulate or wild boar activity (respectively, three, two, and three stands were removed for these criteria). Furthermore, we did not include a unique Andosol site, having high contents of Al_o and Fe_o compared to the other sites, as done by Hall and Thompson (2022).

https://doi.org/10.5194/egusphere-2026-6489
Preprint. Discussion started: 9 November 2026
© Author(s) 2026. CC BY 4.0 License.

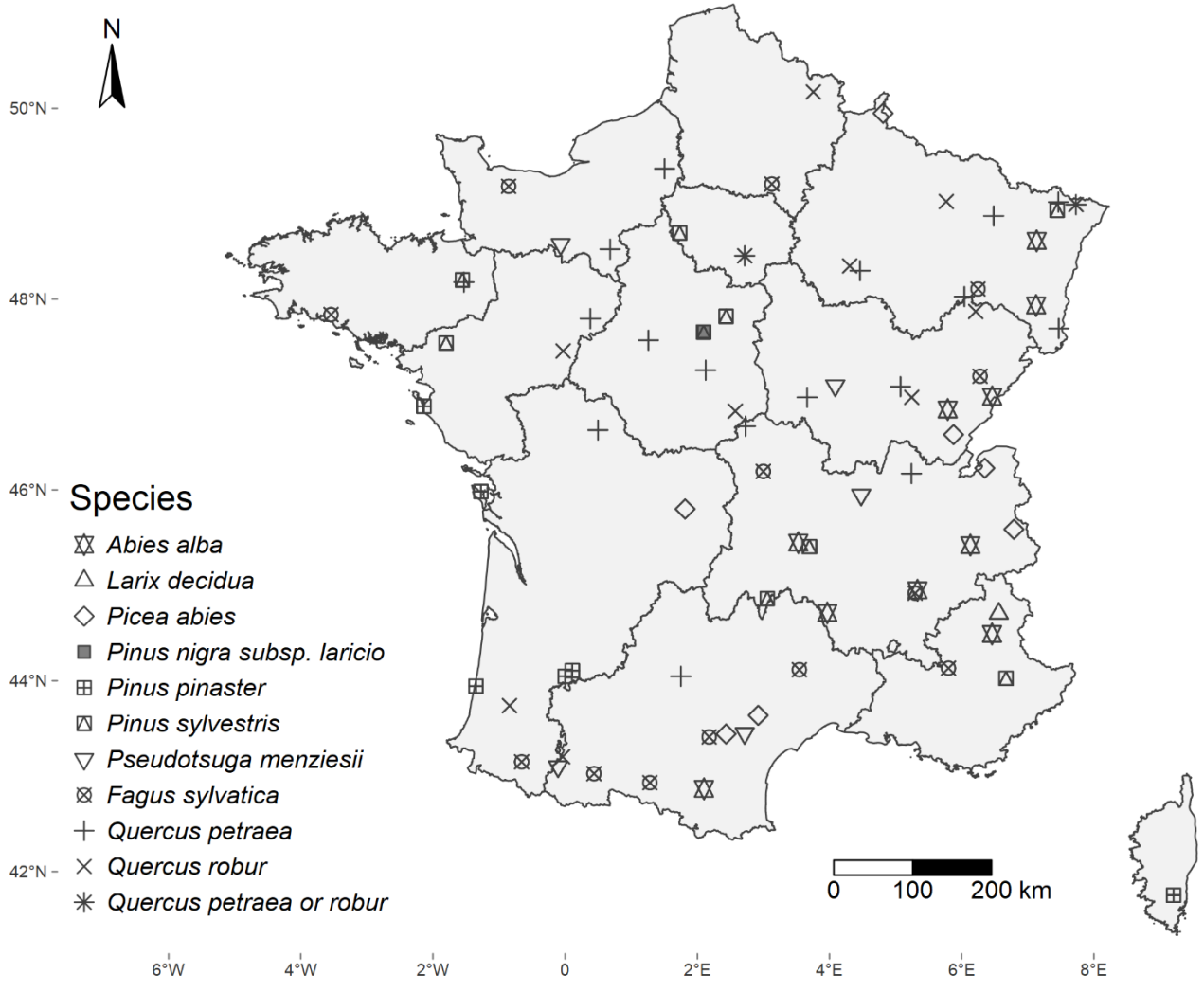


Figure 1: Location of the 80 selected forests stands from the RENECOFOR monitoring network. The 11 main trees cover considered are shown, the seven first ones being conifer species, while the four last are broadleaf species. Background map under the ODbL licence, credits to the OpenStreetMap contributors.

2.2 SOC content, dynamics and pools

For each site, three soil layers depths (0–10, 10–20, and 20–40 cm) and the forest floor layers were sampled at each campaign in five subplot. Each subplot consisted of five sampling points, which were pooled into a composite sample for the soil properties analyses (Jonard et al., 2017). The holorganic layers were sampled using a 30×30 cm frame, and the mineral layers by digging a 50×50 cm hole. The carbon stock of the forest floor layer was also characterised but only used as an explanatory variable (see Section 2.3).

https://doi.org/10.5194/egusphere-2026-6489
Preprint. Discussion started: 9 November 2026
© Author(s) 2026. CC BY 4.0 License.

The samples used for chemical analyses were oven-dried at 35 °C for 24 h. The samples of the forest floor were grinded before performing the chemical analyses, while the mineral soil samples were sieved to < 2 mm. The chemical analyses were performed at the Laboratory of Soil Analyses (INRAe Arras, France). Soil samples with pH $CaCl_2$ > 6 were decarbonated following Harris et al. (2001) prior to the measurement of organic carbon content. The samples were treated by dry combustion (Dumas method – NF ISO 10694, 1995) for forest floor and 0–10 cm soil layers, and by sulfochromic oxidation (Anne method – Anne, 1945; NF X31-109, 1993) for the 10–20 and 20–40 cm soil layers.

For each site, the soil from the five sub-plots per layer has been isovolumetrically pooled for the Rock-Eval® 6 turbo device analysis (Vinci Technologies, France) at ISTeP – UMR 7193 (Sorbonne Université, Paris, France). The Rock-Eval® procedure to assess the fraction of labile and stable C was presented by Soucémarianadin et al. (2018) and was applied to samples from both soil sampling campaigns. It was adapted from Behar et al. (2001), Disnar et al. (2003) and Baudin et al. (2015) for soil samples. For each sample, about 60 mg of ground and dried soil was placed in a stainless-steel pod. As a first step, it underwent a pyrolysis in a N_2 atmosphere during 3 min at 200 °C, and raised at an increase of 30 °C·min^{-1} up to 650 °C. Both the gaseous emissions of hydrocarbon compounds and CO and CO_2 emissions were monitored respectively by a flame ionisation detector and an infrared detector. The second step consisted of an oxidation at laboratory air atmosphere (CO_2 and H_2O previously removed), heated during 1 min at 300 °C, and raised at an increase of 20 °C·min^{-1} up to 850 °C, at which the sample remained during 5 min. The CO and CO_2 emissions were again continuously monitored during this phase with an infrared detector. The Rock-Eval® analysis led to more than 30 measured or estimated parameters, and we used two of them which are of particular interest to proxy the labile and stable organic carbon (Cécillon et al., 2021; Delahaie et al., 2023). The former, associated with the labile organic carbon, is the hydrogen index (HI), which corresponds to the quantity of hydrocarbons released between 200 and 650 °C on the total organic carbon estimated by Rock-Eval®, expressed in mg HC·g^{-1} TOC. The second parameter used as a proxy of SOM stability, T_{50} CO_2 PYR, is the temperature corresponding to the evolution of 50 % of the total amount of CO_2 evolved during the pyrolysis phase. Reproducibility and accuracy of Rock-Eval® parameters published by Pacini et al. (2023) were verified by analysing a reference sample every 10 tests and by performing duplicate analyses at random.

We tested our hypotheses (H1), (H2) and (H3) on SOC content drivers only on data from the second campaign, as some soil properties needed to validate our hypotheses were not estimated during the first campaign (see Section 2.3). SOC content rather than the SOC stock was examined, to avoid introducing the uncertainty related to soil bulk density and stone content measurement that would blur the relationships (Yang et al., 2022). As the Rock-Eval® analyses were performed on pooled samples, we averaged other data available for each of the five subplots per site and soil depth to carry out the statistical analyses.

The annual changes were calculated by dividing the changes in stock levels by the time interval between the two sampling dates, as C variation: $\Delta C = \frac{C_{campaign2} - C_{campaign1}}{Time}$.

https://doi.org/10.5194/egusphere-2026-6489
Preprint. Discussion started: 9 November 2026
© Author(s) 2026. CC BY 4.0 License.

2.3 Climatic, forest and soil characteristics

Twelve variables were included to correlate with SOC content and dynamics (Table 1): two climatic variables, five forest stand variables and five soil variables. Climatic variables refer to the mean annual temperature (in °C) and precipitation (in $dm \cdot year^{-1}$), which were available for each site using the nearest Météo-France stations having a comparable altitude (average distance from site ± standard deviation: 18.4 ± 9.7 km).

Each site was assigned a tree functional type (broadleaf versus conifer) according to the dominant species of each site (Figure 1). Regular litter inputs from the canopy (e.g. leaves, small branches, and a miscellaneous category, including fruits, buds and bark) were collected four times per year in 10 traps of 0.5 m^2 arranged on a 20×20 m grid, between the beginning of the monitoring, and depending on the site, up to 2007 or to the date of the second soil sampling campaign. Following the methodology used by Mao et al. (2019) working on the same dataset, the carbon amount from litter inputs was estimated using the carbon content of the plant organ measured in 1996–2000 or in 2009–2010. Regular inputs from fine roots were considered similar to that from leaves with a fixed ratio of 1:1 for both broadleaf and coniferous stands as done by Mao et al. (2019). Besides regular input from aboveground organs and fine roots, we further estimated irregular litter inputs due to thinning and minor storms, including coarse branches and coarse roots from the available information from tree inventories for each site, calculating the coarse roots carbon inputs using the ratios presented in Cairns et al. (1997).

https://doi.org/10.5194/egusphere-2026-6489
Preprint. Discussion started: 9 November 2026
© Author(s) 2026. CC BY 4.0 License.

Table 1: Description of climatic variables, stand characteristics and soil properties tested as driver of SOC content, hydrogen index and T_{50} CO_2 PYR as well as driver of change in SOC at the decadal time scale. Mean, standard deviation and range of values for the 80 forest plots selected from the RENECOFOR network, after removal of plots affected by disturbances.

Variables available at the stand level

Category	Variable	Mean ± SD [Min - Max]	Unit
Climate	Mean annual temperature (MAT)	10.06 ± 1.97 [4.62 - 13.8]	°C
	Mean annual precipitation (MAP)	9.83 ± 3.04 [5.75 - 21.66]	$dm \cdot year^{-1}$
Stand	Functional group	Broadleaf (n = 41) or Conifer (n = 39)	
	Regular litter	0.35 ± 0.07 [0.16 - 0.50]	$kg \cdot m^{-2} \cdot year^{-1}$
	Irregular litter	0.13 ± 0.07 [0.00 - 0.31]	$kg \cdot m^{-2} \cdot year^{-1}$
	Forest floor carbon stock	1.18 ± 1.16 [0.13 - 6.05]	$kg \cdot m^{-2}$
	Annual stock variation of the forest floor	8.95 ± 29.21 [-50.5 - 134]	$g \cdot m^{-2} \cdot year^{-1}$

Variables available at each soil depth

Category	Variable	0–10 cm	10–20 cm	20–40 cm	Unit
Soil properties	pH	4.74 ± 0.88 [3.72 - 8.36]	4.93 ± 0.92 [4.06 - 8.70]	5.20 ± 1.07 [4.11 - 8.97]	
	Number of sites by pH group	pH < 5: 59; pH ≥ 5: 21	pH < 5: 59; pH ≥ 5: 21	pH < 5: 58; pH ≥ 5: 22	
	Clay proportion	19.57 ± 11.68 [0.1 - 51.9]	18.48 ± 11.76 [0.1 - 55.6]	19.11 ± 13.27 [0.1 - 68.0]	%
	Ca^{2+} + Mg^{2+} content	5.75 ± 9.60 [0 - 52.8]	4.56 ± 9.26 [0 - 48.6]	4.91 ± 9.87 [0 - 44.7]	$cmol^{+} \cdot kg^{-1}$
	Al_o + 0.5 Fe_o content	4.64 ± 3.23 [0.12 - 13.9]	5.25 ± 3.85 [0.10 - 18.9]	5.39 ± 4.04 [0.16 - 20.7]	$g \cdot kg^{-1}$
	Al_o content	2.46 ± 1.98 [0 - 9.71]	2.92 ± 2.43 [0 - 12.1]	3.19 ± 2.78 [0 - 16.0]	$g \cdot kg^{-1}$
	Fe_o content	4.35 ± 3.09 [0.06 - 12.6]	4.65 ± 3.46 [0.09 - 15.9]	4.38 ± 3.14 [0.08 - 15.0]	$g \cdot kg^{-1}$
	Mean total SOC content	50.57 ± 28.93 [8.14 - 180]	24.32 ± 15.73 [1.72 - 79.9]	15.17 ± 11.62 [1.28 - 53.7]	$g \cdot kg^{-1}$
	Mean Hydrogen Index	294 ± 81 [114 - 445]	241 ± 81 [88 - 435]	183 ± 59 [78 - 421]	mg HC·g TOC^{-1}
	T_{50} CO_2 PYR	368 ± 10 [348 - 400]	378 ± 8 [355 - 406]	384 ± 8 [372 - 414]	°C

The forest floor layers were identified following the humus classification of Brêthes et al. (1995) and using the three main categories: OL – organic layer with mainly untransformed plant remains; OF – layer with fragmented plant remains; and OH – layer consisted of more than 70 % of fine organic matter. The carbon stock of each layer was obtained by multiplying its dry mass relative to the surface area by its organic carbon content, and their stocks were summed.

Regarding soil properties, particle size measurements have been done by Robinson pipette and underwater sieving without removal of carbonates (NF X 31-107, 2003), giving three size fractions (clay: ≤ 2 µm; silt: 2–63 µm; sand: 63–2000 µm). Exchangeable Ca and Mg were extracted using a solution of barium chloride at 0.1 $mol \cdot l^{-1}$ in a 1:10 mass/volume ratio (NF ISO 11260, 1994), then measured by flame atomic absorption spectroscopy. The oxalate-extracted aluminium (Al_o) and iron (Fe_o) were measured with the Tamm method in the dark (NF ISO 22036, 2009). Soil water pH was determined with a glass electrode in a solution of 1 volume of soil in 5 volumes of deionised water (NF ISO 10390, 2004). We considered the pH as a grouping variable, choosing a threshold at pH 5.0, as Guidi et al. (2025) – with two groups, pH < 5, and pH ≥ 5. It matches

https://doi.org/10.5194/egusphere-2026-6489
Preprint. Discussion started: 9 November 2026
© Author(s) 2026. CC BY 4.0 License.

the shift between the Al forms, from a majority of Al^{3+} at pH < 5 to other forms of Al at pH > 5 (Sparks, 2003) and also integrates the effects faunal and microbial communities (Desie et al., 2021). Furthermore, such pH-based classification captures soil functional shift, from an effect of reactive minerals (Al_o and Fe_o) on carbon content at lowest pH, to that of exchangeable cations at highest pH (Rasmussen et al., 2018).

All the soil properties were characterised for each soil layer. As mentioned previously for SOC content, the values of the subplots were averaged at the scale of the soil depth and site. Only the data of the second campaign were used for the carbon content, as some variables, such as Al_o and Fe_o were not available for the first campaign. The reactive minerals were expressed as $Al_o + 0.5\ Fe_o$, to consider their difference in molecular weight (Wagai et al., 2020).

2.4 Statistical analyses

We performed Bayesian modelling to explore the link between soil storage and abiotic and biotic variables, as in this framework, the estimates are valid even for small sample sizes (McElreath, 2020). To identify how carbon content and its variations over 15 years respond to the selected explanatory variables, we performed generalised linear models. For SOC, HI and T_{50} CO_2 PYR, a model was made for each soil depth layer (0–10, 10–20, and 20–40 cm) with 13 explanatory variables included (Table 1). Among those, we included the interactions between the pH class and the following three variables: clay content, $Al_o + 0.5\ Fe_o$ content, $Ca^{2+} + Mg^{2+}$ content, as the effect of these variables was expected to be strongly conditioned by the pH. All continuous explanatory variables were normalised following $\frac{x_i - \bar{x}}{\sigma}$, with $\bar{x}$ and σ the average and standard deviation of x.

2.4.1 Observed values of SOC, HI, and T_{50} CO_2 PYR

We chose a Beta distribution for SOC content and HI, as shown in Eq. (1), as these variables can be expressed as proportions bounded between 0 and 1 (kg C·kg^{-1} soil and g HC·g^{-1} TOC respectively) and transformed with a logit link: $\text{logit}(y) = \log\left(\frac{y}{1-y}\right)$. The Beta distribution is defined as $f(y) = \frac{y^{\alpha-1}(1-y)^{\beta-1}}{\mathcal{B}(\alpha,\beta)}$, with $\alpha = \mu \times \phi$ and $\beta = (1-\mu) \times \phi$, where y is the response variable, f the density function, μ the mean, ϕ a positive precision parameter, and B the beta function, defined as $\mathcal{B}(a,b) = \frac{\Gamma(a)\Gamma(b)}{\Gamma(a+b)}$, with Γ is the gamma function – $\Gamma(n) = (n-1)!$.

The Bayesian models are described as:

$$\begin{aligned} \text{C-content}_i \text{ or } \text{HI}_i &\sim \text{Beta}(\alpha_i, \beta_i) \\ \alpha_i &= \mu_i \times \phi \\ \beta_i &= (1-\mu_i) \times \phi \\ \text{logit}(\mu_i) &= \beta_0 + \sum_{k=1}^{13} \beta_k\, x_{ki} \\ \beta_{1,\dots,13} &\sim \mathcal{N}(0,2) \end{aligned} \quad (1)$$

https://doi.org/10.5194/egusphere-2026-6489
Preprint. Discussion started: 9 November 2026
© Author(s) 2026. CC BY 4.0 License.

Where β_0 is the intercept, $\beta_{1,\dots,13}$ are the parameters of the explanatory variables x; Beta(), and $\mathcal{N}()$ represent respectively a Beta, and Normal distribution.

We used $\mathcal{N}(0,2)$ for the $\beta_{1,\dots,13}$ parameters rather than wider or uniform ones. We chose this prior given that the predictor variables had been standardised where they were continuous and that the response variable had been transformed using a logit link function. The priors should not restrain the parameters without giving too much weight to the distribution tails, which can lead to high estimate values in logit links (McElreath, 2020). Having no a priori hypothesis about the intercept and the ϕ parameters, we left the function default settings.

For T_{50} CO_2 PYR, we performed a model based on a Normal distribution as shown in Eq. (2). A wider prior for the β_k coefficients was used as the response variable was not transformed. We kept the default priors for β_0 and σ:

$$\begin{aligned} T_{50}\ CO_2\ PYR_i &\sim \mathcal{N}(\mu_i, \sigma) \\ \mu_i &= \beta_0 + \sum_{k=1}^{13} \beta_k x_{ki} \\ \beta_{1,\dots,13} &\sim \text{StudentT}(3,0,2) \end{aligned} \qquad (2)$$

Where StudentT() represents a Student's *t* distribution

2.4.2 Annual variation of SOC, HI, and T_{50} CO_2 PYR

SOC, HI and T_{50} CO_2 PYR variation can be positive and negative. Therefore, we chose the Student's *t* distribution as described in Eq. (3), which is also more robust to influential data points, compared to a Normal distribution (McElreath, 2020). Given that most of the recent carbon is found in the topsoil (Balesdent et al., 2018) and that the changes occurred mainly in the 0–10 cm layer (as shown by the results), we present here only the models relating to the topsoil.

The Student's *t* distribution is defined as: $f(y) = \frac{\Gamma((\nu+1)/2)}{\Gamma(\nu/2)} \frac{1}{\sqrt{\nu\pi}\sigma} (1 + \frac{1}{\nu}(\frac{y-\mu}{\sigma})^2)^{-(\nu+1)/2}$.

Where $\nu > 1$ are the degrees of freedom, and σ is the standard deviation.

This model describing C content change considered the forest floor stock variations instead of forest floor stock of the second campaign. Indeed, C may be transferred from forest floor to mineral soil, depending on humus type (Zanella et al., 2018). It also considered the mean C–content of the two campaigns, instead of the stock from the second campaign, as C–content variation can also be impacted by the content itself in a context of steady-state (Stewart et al., 2007). This averaging was advised by Oldham (1962) in case of two repeated measurements, to avoid a spurious correlation between SOC content and its variation. Finally, as for the previous models, we tested the interaction effect between the pH class and clay content, $Al_o + 0.5\ Fe_o$ content, and $Ca^{2+} + Mg^{2+}$ content.

The Bayesian models are described as:

$$\begin{aligned} \Delta C_i &\sim \text{StudentT}(\nu, \mu_i, \sigma) \\ \mu_i &= \beta_0 + \sum_{k=1}^{14} \beta_k x_{ki} \\ \beta_{1,\dots,14} &\sim \mathcal{N}(0,2) \end{aligned} \qquad (3)$$

https://doi.org/10.5194/egusphere-2026-6489
Preprint. Discussion started: 9 November 2026
© Author(s) 2026. CC BY 4.0 License.

As for the Beta models, we used a Normal distribution for the $\beta_{1,\dots,14}$ parameters, as the continuous variables were scaled and the response variable had a low amplitude. Having no a priori hypothesis about the intercept, ν and σ values, we left the function default settings. Furthermore, we proposed a second model for the variation of SOC, using the same variables as before, but which also integrated the HI and T_{50} CO_2 PYR of the first campaign. That way, it allowed us to verify if the variations of SOC between the two sampling campaigns were mainly driven by the soil, stand, and climate variables, or were also influenced by the nature of the soil carbon. The two competing models for SOC variation (with or without the HI and T_{50} CO_2 PYR variables) were weighted using the Leave-One-Out Cross-Validation based model comparison described by Sivula et al. (2025) to estimate the best model.

For each response variable (SOC content, HI, T_{50} CO_2 PYR, and their variation), we tested the effect of the depth layer as specified in Eq. (4), using the same family distribution used for the full models. We only considered the effect of the layer, as well as the identity of the site, using as formula:

$$\begin{aligned} \text{Response}_i &= \begin{bmatrix}\beta_1\\ \beta_2\\ \beta_3\end{bmatrix}\begin{bmatrix}\text{Layer } 0-10\text{cm}_i & 0 & 0\\ 0 & \text{Layer } 10-20\text{cm}_i & 0\\ 0 & 0 & \text{Layer } 20-40\text{cm}_i\end{bmatrix} + \alpha_{Site[i]} \\ \alpha_{Site[i]} &\sim \mathcal{N}(0,\sigma) \\ \sigma &\sim \text{HalfStudentT}(3,0,2.5) \end{aligned} \quad (4)$$

The other priors were the same as those used in the respective models. These models were not adequate after checking model assumptions, but we still used them to verify an overall effect of the layer depth.

The intercept was based on the broadleaf stands and soil pH ≥ 5. Therefore, the coefficients for clay, Al_o + 0.5 Fe_o, and Ca^{2+} + Mg^{2+} content were based on the soil pH ≥ 5 class, and the effects for pH < 5 were coded as contrasts. But we want to know if the variables of interest (clay content, Al_o + 0.5 Fe_o, and Ca^{2+} + Mg^{2+} content) had an effect for both pH classes. Therefore, we present the total effects for pH < 5, i.e. calculated for each iteration as the coefficient for pH ≥ 5 + the coefficient of the contrast for pH < 5, from which the median and CI were computed.

For the SOC content and HI models, the coefficients were exponentiated to compute the odds ratios, as the response variables were expressed in logits. It allows the intercept to be converted at the data scale and makes the parameters to have a multiplicative effect on the intercept, modulated by the factor if it is discrete, or by their values if it is continuous. Examples of the calculations are expressed in the related tables legends (Table 2 and Table 3).

The median values of the posterior distributions of the parameters' coefficients are expressed, as well as the low and high equal-tailed intervals (ETI) at 95 % by default in brackets. An effect different to 0 or exp(0) at 95 % was considered "significant". Thereafter, we will refer to the ETI as credible intervals (CI). The CI at 90 % are sometimes shown to highlight some tendencies but are specified as 90%CI if so. To verify the validity of the models, we estimated the quantile residuals (Dunn and Smyth, 1996) using the median predictions. In rare occasions, models failed in some diagnostics, but the deviations were considered sufficiently minor and should not have major effect on the validity of the parameters' values.

The data processing and analyses have been carried out with R version 4.5.2 (R Core Team, 2025) on RStudio (v. 2026.01.0+392 – Posit team, 2025). We used the *brms* package (v. 2.23.0 – Bürkner, 2017) for the data analyses, which

https://doi.org/10.5194/egusphere-2026-6489
Preprint. Discussion started: 9 November 2026
© Author(s) 2026. CC BY 4.0 License.

rely on the Stan program (v. 2.37.0 – Stan Development Team, 2024) through the *cmdstanr* package (v. 0.9.0 – Gabry et al., 2025). Stan uses the No-U-Turn sampler, an extension of the Hamiltonian Monte Carlo algorithm which converges more efficiently than other Monte Carlo algorithms (e.g. Metropolis and Gibbs – Hoffman and Gelman, 2014). Four independent Markov chains were estimated per model. They were composed of 2,000 iterations, including 1,000 warm-up ones (iterations used to internally tune the sampling efficiency). After warmup, each iteration was kept, yielding to 4,000 samples from which the posteriors were drawn. We used the *DHARMa* package (v. 0.5.0 – Hartig, 2026) to compute the quantile residuals.

3. Results

3.1 Soil carbon content

SOC content decreased significantly with depth, from an average of 50.6 ± 28.9 g C·kg^{-1} soil (mean ± standard deviation) at 0–10 cm depth, to 24.3 ± 15.7 g·kg^{-1} at 10–20 cm, and 15.2 ± 11.6 g·kg^{-1} at 20–40 cm. This decrease was confirmed by the layer depth model, with an odds ratio (OR) of 0.47 [0.44, 0.50] for SOC content between the 0–10 cm and the 10–20 cm layers, and an OR of 0.61 [0.56, 0.67] between 10–20 cm and the 20–40 cm layers.

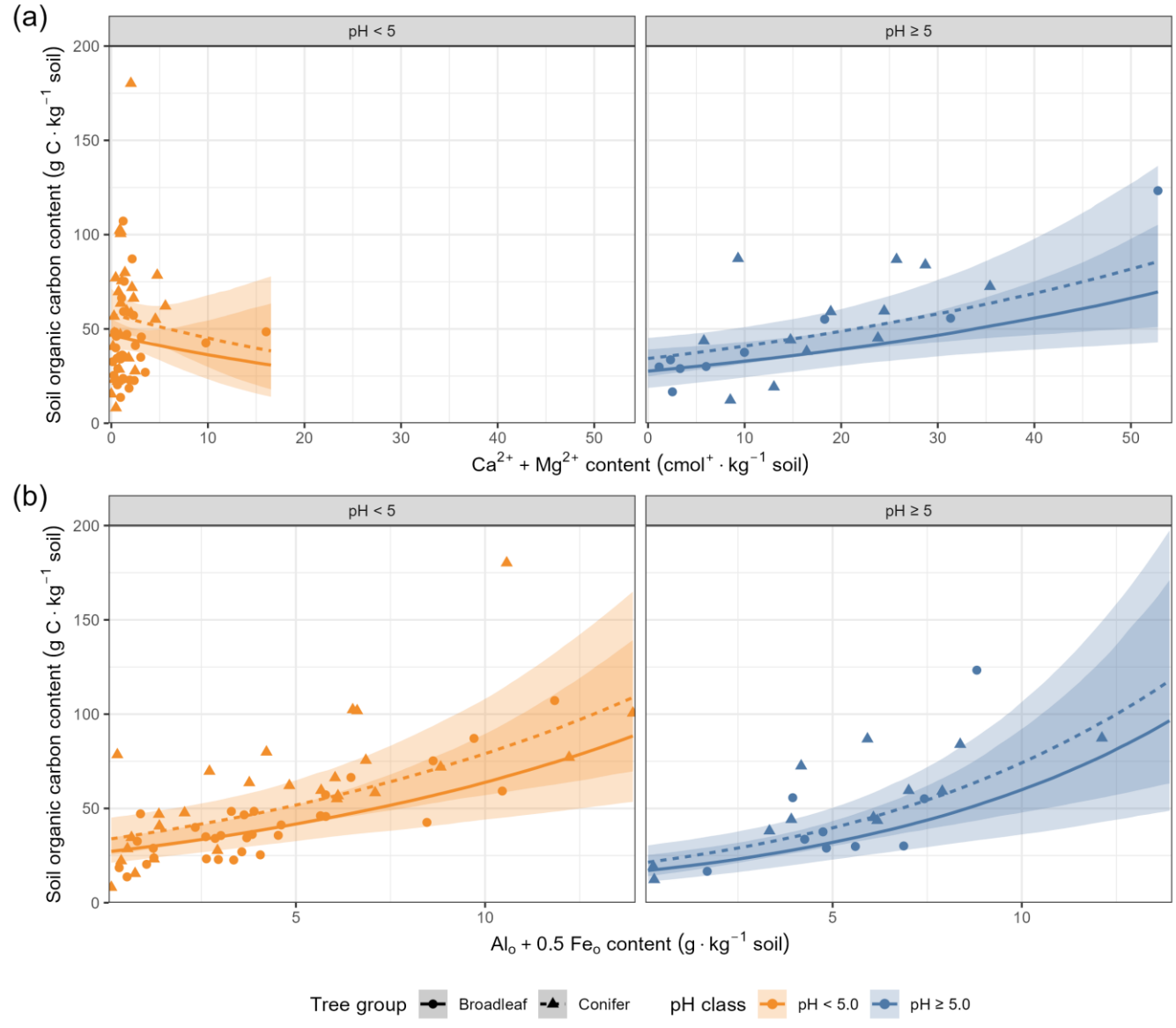
For the full models, Ca^{2+} + Mg^{2+} in sites with pH ≥ 5 and Al_o + 0.5 Fe_o (Figure 2 a and Figure 2 b) for both pH groups significantly increased SOC content for the three layers depth, with a tendency towards a greater effect for the 10–20 cm and 20–40 cm layers compared to the 0–10 cm layer (Table 2). Other soil effects were observed to increase SOC content but only for the two first layers: the pH group, increasing SOC content (tendency for the 0–10 cm layer with an OR of 1.34 [90%CI 1.01, 1.78], and significantly for the 10–20 cm layer with an OR of 1.45 [1.02, 2.02]), and clay content for the 0–10 cm layer in the pH < 5 sites (OR 1.21 [90%CI 1.01, 1.43]). Some stand and climate variables impacted SOC content, depending on layer depth, mainly at 90%CI. For the 0–10 cm layer, the coniferous stands had more SOC content compared to broadleaf stands (OR 1.26 [90%CI 1.03, 1.54]), and an increase in mean annual temperature decreased SOC content (OR 0.91 [90%CI 0.83, 1.00]). For the 10–20 cm layer, no stand nor climate variable impacted SOC content. For the 20-40 cm layer, two stand variables decreased SOC content: the average coarse branches and roots inputs, expressed as irregular litter (OR 0.88 [0.81, 0.96]), and the carbon stock of the forest floor (OR 0.90 [90%CI 0.82, 0.99]). As a relationship between SOC in the 20-40 cm layer and forest floor was rather unlikely as none was observed in the topsoil layers, we consider these relationships probably spurious and will not discuss them further.

https://doi.org/10.5194/egusphere-2026-6489
Preprint. Discussion started: 9 November 2026
© Author(s) 2026. CC BY 4.0 License.

Table 2: Results of the models of the soil organic carbon content for the 0–10, 10–20, and 20–40 cm soil depth layers. These models used a logit link, and the coefficients are expressed as odds ratios (i.e. the parameters are exponentiated, which makes the effects multiplicative). The median odds ratios are shown, with the 95 % credible intervals in square brackets; the parameters different from 1 – i.e. exp(0) – at 95 % credible intervals are in bold, and those different from 1 at 90 % are underlined. ϕ is the other parameter estimated for the Beta distribution. An odds ratio > 1 means the effect is positive, while an odds ratio < 1 states a negative effect. Odds ratios are multiplicative relatively to the intercept. For instance, the prediction for a broadleaf site with pH ≥ 5 and a value of Al_o + 0.5 Fe_o of 0.5 standard deviation higher at 0–10 cm, is $0.03 \times 1.26 \times 1.53^{0.5} = 0.05$ kg SOC·kg^{-1} soil, keeping all other explanatory variables at their mean.

	0–10 cm	10–20 cm	20–40 cm
Intercept (broadleaf sites with pH ≥ 5)	0.03 [0.02, 0.04]	0.02 [0.01, 0.02]	0.01 [0.01, 0.01]
Functional group; Conifers	1.26 [0.98, 1.61]	1.10 [0.89, 1.38]	1.00 [0.81, 1.25]
Regular litter	0.98 [0.89, 1.08]	1.05 [0.96, 1.16]	1.01 [0.91, 1.12]
Irregular litter	0.99 [0.90, 1.09]	0.95 [0.87, 1.04]	**0.88 [0.81, 0.96]**
Forest floor carbon stock	1.04 [0.93, 1.15]	0.98 [0.87, 1.08]	0.90 [0.80, 1.01]
Mean annual temperature	0.91 [0.82, 1.02]	0.94 [0.85, 1.05]	0.95 [0.85, 1.06]
Mean annual precipitation	0.95 [0.86, 1.06]	1.02 [0.91, 1.13]	1.08 [0.97, 1.20]
Sites with pH < 5	1.34 [0.96, 1.91]	**1.45 [1.02, 2.02]**	1.26 [0.51, 2.98]
Clay content; sites with pH ≥ 5	0.99 [0.86, 1.15]	0.99 [0.86, 1.14]	0.94 [0.83, 1.06]
Clay content; sites with pH < 5	1.21 [0.98, 1.48]	0.94 [0.79, 1.10]	0.85 [0.70, 1.05]
Al_o + 0.5 Fe_o; sites with pH ≥ 5	**1.53 [1.24, 1.87]**	**1.75 [1.46, 2.09]**	**1.88 [1.56, 2.25]**
Al_o + 0.5 Fe_o; sites with pH < 5	**1.34 [1.16, 1.55]**	**1.49 [1.35, 1.64]**	**1.44 [1.31, 1.56]**
Ca^{2+} + Mg^{2+}; sites with pH ≥ 5	**1.19 [1.05, 1.35]**	**1.28 [1.16, 1.42]**	**1.27 [1.13, 1.42]**
Ca^{2+} + Mg^{2+}; sites with pH < 5	0.78 [0.46, 1.30]	1.32 [0.72, 2.21]	1.13 [0.15, 7.28]
ϕ	175 [123, 241]	387 [268, 535]	573 [397, 779]

https://doi.org/10.5194/egusphere-2026-6489
Preprint. Discussion started: 9 November 2026
© Author(s) 2026. CC BY 4.0 License.



345 **Figure 2: Model estimated effect of (a): exchangeable calcium and magnesium, and (b): content oxalate-extracted aluminium + 0.5 iron content on soil organic carbon content for the 0–10 cm depth layer depending on pH class and tree functional group. The left panels are the relationship for the pH < 5 soils (orange), the right panels the pH ≥ 5 soils (blue). The broadleaf and coniferous stands are represented separately (solid lines and circles: broadleaf, dotted lines and triangles: conifer). The ribbons show the credible intervals at 95 % of the coefficients.**

350 **3.2 Rock-Eval® indices**

The Hydrogen Index (HI) represents the quantity of hydrocarbon per g of organic carbon (mg HC·g^{-1} TOC) and is assumed to be a proxy of poorly decomposed organic matter (Barré et al., 2024). It decreased significantly with layer depth, with 283.8 ± 79.2 mg HC·g^{-1} TOC at 0–10 cm, 223.3 ± 76.5 mg HC·g^{-1} TOC at 10–20 cm, and 167.7 ± 61.0 mg HC·g^{-1} TOC at

https://doi.org/10.5194/egusphere-2026-6489
Preprint. Discussion started: 9 November 2026
© Author(s) 2026. CC BY 4.0 License.

20–40 cm. The depth layer model confirmed the reduction of HI between the 0–10 cm and 10–20 cm layers (OR 0.72 [0.67, 0.78]), and between the 10–20 and 20–40 cm layers (OR 0.69 [0.64, 0.76]).

Compared to SOC content, the influence of other variables had a less clear pattern with soil depth. Overall, the functional group had a significant effect on HI, with a lower hydrocarbon concentration in coniferous stands compared to broadleaf ones for all depth layers (Table 3). For the two first layers, sites with pH < 5 had higher HI (OR 1.71 [1.36, 2.15] for the 0–10 and 10–20 cm layers respectively), and regular litter inputs (leaves, small roots and branches, and other organs) reduced it (OR 0.90 [0.84, 0.96] for the 0–10 cm layer; Figure 3 a). However, this negative effect of litter inputs seemed to be driven by coniferous sites. HI tended to decrease along litter inputs in conifer sites while there was no relationship in broadleaf sites (Figure 3 a).

Other soil properties influenced HI, but with less clear patterns. In the more acidic sites, clay content significantly reduced HI for the two deepest layers (OR 0.69 [0.59, 0.82] and 0.62 [0.52, 0.75] for the 10–20 and 20–40 cm layers respectively). Furthermore, pH class had an influence by mediating the relationship between HI and other soil properties. Thus, Al_o + 0.5 Fe_o had a significant negative effect on HI in more acidic sites in the surface layer (OR 0.87 [0.77, 0.97]; Figure 3 b), but this was not observed in subsequent layers. Conversely, the negative effect of Al_o + 0.5 Fe_o was present in the deepest layer for the pH ≥ 5 sites (OR 0.78 [0.60, 0.98]). Basic cations also increased HI for the 20–40 cm, but not in the other layers. For the more acidic sites, the effect of cations was not consistent, despite a high positive relationship with HI in the 10–20 cm layer.

https://doi.org/10.5194/egusphere-2026-6489
Preprint. Discussion started: 9 November 2026
© Author(s) 2026. CC BY 4.0 License.

Table 3: Results of the models of the hydrogen index for the 0–10, 10–20, and 20–40 cm soil layers depth. These models used a logit link, and the coefficients are expressed as odds ratios (i.e. the parameters are exponentiated, which makes the effects multiplicative). An odds ratio > 1 means the effect is positive, while an odds ratio < 1 states a negative effect which are multiplicative relatively to the intercept. For instance, the prediction for a site with pH < 5 and a value of Al_o + 0.5 Fe_o of 0.5 standard deviation higher at 0–10 cm, is $0.31 \times 1.71 \times 0.87^{0.5} = 0.49$ g HC·g^{-1} TOC, keeping all other explanatory variables at their mean. The median odds ratios are shown, with the 95 % credible intervals in square brackets; the parameters different from 1 – i.e. exp(0) – at 95 % credible intervals are in bold, and those different from 1 at 90 % are underlined. ϕ is the other parameter estimated for the Beta distribution.

	0–10 cm	10–20 cm	20–40 cm
Intercept (broadleaf sites with pH ≥ 5)	0.31 [0.25, 0.37]	0.22 [0.17, 0.29]	0.16 [0.13, 0.21]
Functional group; Conifers	**0.70 [0.59, 0.83]**	**0.69 [0.54, 0.87]**	**0.77 [0.61, 0.99]**
Regular litter	**0.90 [0.84, 0.96]**	**0.90 [0.82, 0.99]**	0.93 [0.84, 1.02]
Irregular litter	1.01 [0.95, 1.08]	1.02 [0.93, 1.11]	0.99 [0.90, 1.08]
Forest floor carbon stock	1.04 [0.97, 1.12]	**1.11 [1.01, 1.21]**	0.98 [0.88, 1.08]
Mean annual temperature	0.98 [0.91, 1.06]	1.05 [0.94, 1.17]	**1.14 [1.03, 1.27]**
Mean annual precipitation	1.00 [0.93, 1.09]	1.09 [0.98, 1.22]	1.11 [0.99, 1.25]
Sites with pH < 5	**1.71 [1.36, 2.15]**	**2.39 [1.74, 3.31]**	1.45 [0.61, 3.24]
Clay content; sites with pH ≥ 5	1.03 [0.90, 1.18]	1.09 [0.92, 1.32]	0.94 [0.82, 1.07]
Clay content; sites with pH < 5	0.96 [0.83, 1.11]	**0.69 [0.59, 0.82]**	**0.62 [0.52, 0.75]**
Al_o + 0.5 Fe_o; sites with pH ≥ 5	0.90 [0.74, 1.07]	0.82 [0.62, 1.04]	**0.78 [0.60, 0.98]**
Al_o + 0.5 Fe_o; sites with pH < 5	**0.87 [0.77, 0.97]**	0.96 [0.84, 1.09]	1.02 [0.91, 1.12]
Ca^{2+} + Mg^{2+}; sites with pH ≥ 5	0.96 [0.87, 1.06]	1.06 [0.92, 1.21]	**1.19 [1.04, 1.36]**
Ca^{2+} + Mg^{2+}; sites with pH < 5	0.99 [0.69, 1.38]	**2.61 [1.49, 4.48]**	1.26 [0.21, 7.61]
ϕ	89.2 [62.4, 123.8]	53.8 [37.3, 73.2]	60.8 [43.4, 84.7]

https://doi.org/10.5194/egusphere-2026-6489
Preprint. Discussion started: 9 November 2026
© Author(s) 2026. CC BY 4.0 License.

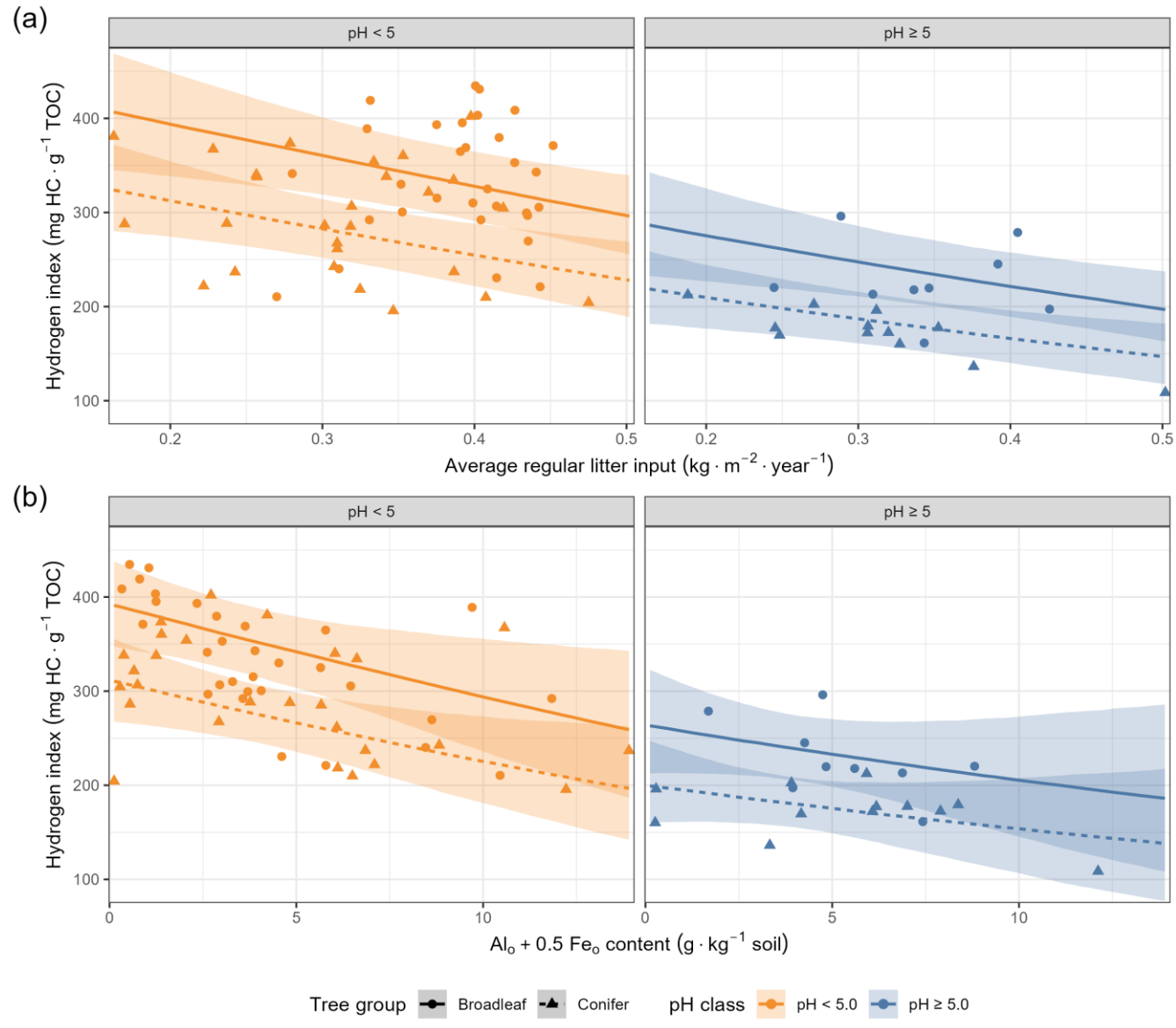


Figure 3: Model estimated effect of (a): average regular litter input (leaves, fine roots, small branches, miscellaneous litter), and (b): oxalate-extracted aluminium + 0.5 iron content on hydrogen index for the 0–10 cm depth layer depending on pH class and tree functional group. The left panels are the relationship for the pH < 5 soils (orange), the right panels the pH ≥ 5 soils (blue). The broadleaf and coniferous stands are represented separately (solid lines and circles: broadleaf, dotted lines and triangles: conifer). The ribbons show the credible intervals at 95 % of the coefficients.

T_{50} CO_2 PYR is the temperature at which 50 % of the CO_2 was emitted during the pyrolysis phase and is positively correlated with stable carbon proportion. T_{50} CO_2 PYR significantly increased with depth, from 367 ± 10 °C at 0–10 cm,

https://doi.org/10.5194/egusphere-2026-6489
Preprint. Discussion started: 9 November 2026
© Author(s) 2026. CC BY 4.0 License.



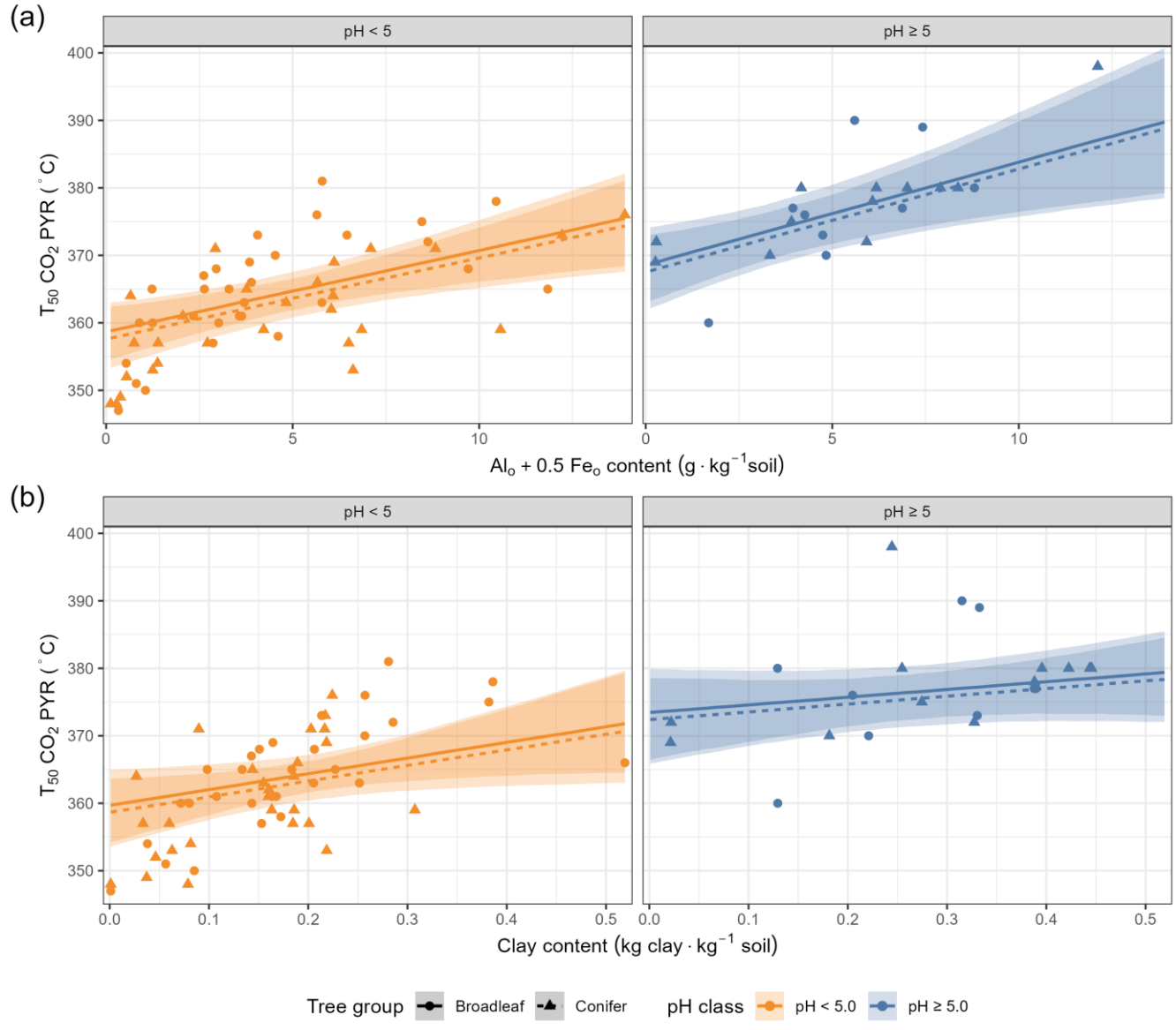
EGUsphere
Preprint repository

378 ± 9 °C at 10–20 cm, and 384 ± 9 °C at 20–40 cm. The depth layer model confirmed it, with a median increase of 10.9 °C [9.2, 12.6] between the 0–10 cm and 10–20 cm layers, and of 6.3 °C [4.6, 8.0] between the 10–20 cm and 20–40 cm layers. Only soil characteristics influenced the T_{50} CO_2 PYR, and this was the case only for the 0–10 cm and 10–20 cm layers. Sites with pH < 5 had a significantly lower T_{50} CO_2 PYR than sites with pH ≥ 5 (-11.5 °C [-16.2, -6.2] for the 0–10 cm layer, -4.9 °C [-10.7, -0.3] for the 10–20 cm layer). For both pH groups, Al_o + 0.5 Fe_o content increased T_{50} CO_2 PYR with the same order of magnitude (for the 0–10 cm layer, 4.93 [1.90, 8.06] for the pH ≥ 5 sites, and 3.91 [1.67, 6.05] for the pH < 5 sites; Figure 4 a). This effect was lower in the 10–20 cm layer but was still significant (2.85 [0.04, 6.25] for the pH ≥ 5 sites, 2.34 [0.23, 4.46] for the pH < 5 sites). Additionally, clay content also increased T_{50} CO_2 PYR for the more acidic sites (2.71 [0.22, 5.47] for the 0–10 and 10-20 cm layers; Figure 4 b).

Table 4: Results of the models of the T_{50} CO_2 PYR for the 0–10, 10–20, and 20–40 cm soil layers depth. The medians are shown, with the 95 % credible intervals in square brackets; the parameters different from 0 at 95 % credible intervals are in bold, and those different from 0 at 90 % are underlined. σ is the other parameter estimated for the Normal distribution. The parameters are given in absolute changes in °C.

	0–10 cm	10–20 cm	20–40 cm
Intercept (broadleaf sites with pH ≥ 5)	375.6 [371.3, 379.8]	381.4 [377.2, 386.1]	384.9 [381.1, 388.9]
Functional group; Conifers	-0.99 [-4.12, 1.85]	-0.15 [-3.30, 2.78]	1.91 [-1.29, 6.54]
Regular litter	0.30 [-1.22, 1.79]	0.31 [-1.30, 1.90]	0.14 [-1.78, 2.08]
Irregular litter	0.02 [-1.44, 1.42]	-0.98 [-2.67, 0.71]	-1.19 [-3.23, 0.57]
Forest floor carbon stock	-0.37 [-1.93, 1.17]	-0.46 [-2.27, 1.21]	0.59 [-1.27, 2.51]
Mean annual temperature	-0.46 [-2.15, 1.16]	-0.48 [-2.36, 1.35]	0.48 [-1.44, 2.44]
Mean annual precipitation	-0.77 [-2.58, 0.99]	-0.55 [-2.58, 1.52]	0.16 [-1.96, 2.34]
Sites with pH < 5	**-11.46 [-16.22, -6.21]**	**-4.87 [-10.67, -0.27]**	-2.14 [-6.92, 1.28]
Clay content; sites with pH ≥ 5	1.33 [-0.84, 3.62]	0.75 [-1.57, 3.05]	0.02 [-2.19, 2.17]
Clay content; sites with pH < 5	**2.71 [0.22, 5.47]**	**2.61 [0.05, 5.27]**	1.13 [-1.83, 4.37]
Al_o + 0.5 Fe_o; sites with pH ≥ 5	**4.93 [1.90, 8.06]**	**2.85 [0.04, 6.25]**	0.45 [-2.11, 3.28]
Al_o + 0.5 Fe_o; sites with pH < 5	**3.91 [1.67, 6.05]**	**2.34 [0.23, 4.46]**	0.92 [-1.28, 3.16]
Ca^{2+} + Mg^{2+}; sites with pH ≥ 5	-0.09 [-2.01, 1.84]	0.46 [-1.67, 2.65]	1.83 [-0.54, 4.19]
Ca^{2+} + Mg^{2+}; sites with pH < 5	-0.32 [-5.04, 4.00]	-0.70 [-7.86, 3.91]	2.48 [-2.36, 8.52]
σ	6.05 [5.11, 7.30]	7.07 [6.00, 8.44]	8.21 [7.04, 9.72]

https://doi.org/10.5194/egusphere-2026-6489
Preprint. Discussion started: 9 November 2026
© Author(s) 2026. CC BY 4.0 License.



405

Figure 4: Model estimated effect of (a): oxalate-extracted aluminium + 0.5 iron content, and (b): clay content on T_{50} CO_2 PYR for the 0–10 cm depth layer depending on pH class and tree functional group. The left panels are the relationships for the pH < 5 soils (orange), the right panels the pH ≥ 5 soils (blue). The broadleaf and coniferous stands are represented separately (solid lines and circles: broadleaf, dotted lines and triangles: conifer). The ribbons show the credible intervals at 95 % of the coefficients.

410 **3.3 Soil organic carbon and RE indices annual variations**

The changes of soil organic carbon between the two sampling campaigns occurred nearly exclusively in the 0–10 cm layer, with an average annual increase of 0.36 ± 0.72 $g \cdot kg^{-1} \cdot year^{-1}$, compared to a negligible average loss for the 10–20 and 20–40 cm layers in comparison (-0.01 ± 0.22 $g \cdot kg^{-1} \cdot year^{-1}$ and -0.04 ± 0.17 $g \cdot kg^{-1} \cdot year^{-1}$, respectively). This was confirmed by

https://doi.org/10.5194/egusphere-2026-6489
Preprint. Discussion started: 9 November 2026
© Author(s) 2026. CC BY 4.0 License.

the depth layer model with a median annual variation of 0.23 [0.18, 0.29] $g \cdot kg^{-1} \cdot year^{-1}$ for the 0-10 layer, against 0.00 [-0.04, 0.04] and -0.03 [-0.07, 0.00] for the two other ones. As stated in the Material and Methods and given the minimal variations in SOC in the 10–20 and 20–40 cm layers, only the annual variation of the 0–10 cm layer was analysed in greater details.

For the first model of SOC content variation, only three variable affected the annual variations of SOC content (Table 5): the tree functional group, with a significant increase of SOC content in coniferous sites compared to broadleaf ones (0.45 [0.13, 0.79]), the annual stock variation of the forest floor, which had a negative effect on the SOC variation (-0.19 [-0.35, -0.07]; Figure 5 a), and $Al_o + 0.5\ Fe_o$ content, which increased SOC content for pH ≥ 5 sites at 90 % credible intervals (0.29 [90%CI 0.01, 0.59]; Figure 5 b). For the model with the added Rock-Eval® parameters, the Hydrogen Index had a significant negative effect on the SOC content variation (-0.34 [-0.62, -0.07]; Figure 6), and the annual stock variation of the forest floor still had a negative effect as for the previous model (-0.16 [-0.31, -0.04]). However, neither the tree functional group nor oxalate-extracted metals were significant anymore, whether at 95 or 90 % credible intervals. The other variables did not have any effect, including the T_{50} CO_2 PYR, at 0.01 [-0.23, 0.25].

https://doi.org/10.5194/egusphere-2026-6489
Preprint. Discussion started: 9 November 2026
© Author(s) 2026. CC BY 4.0 License.

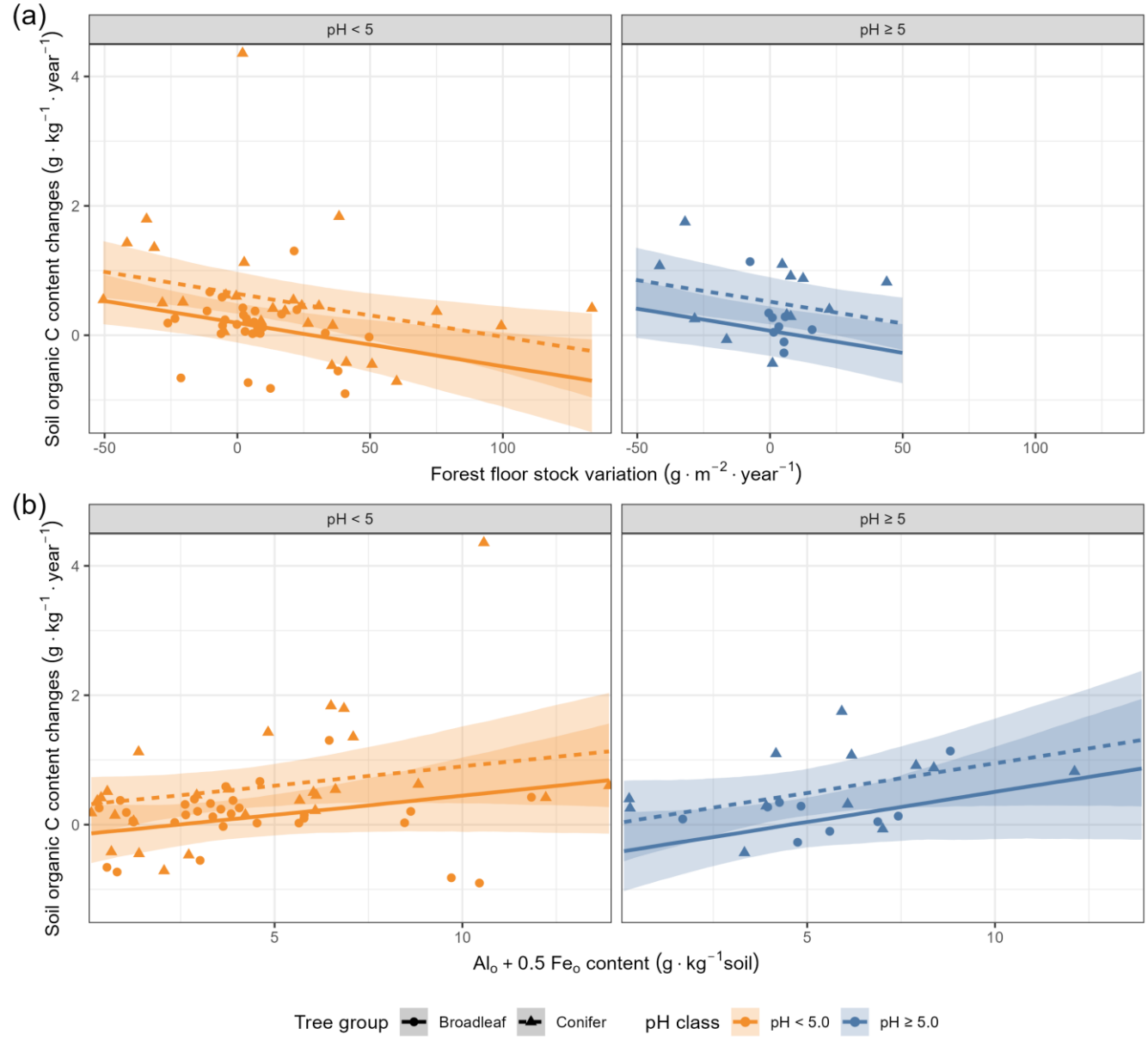
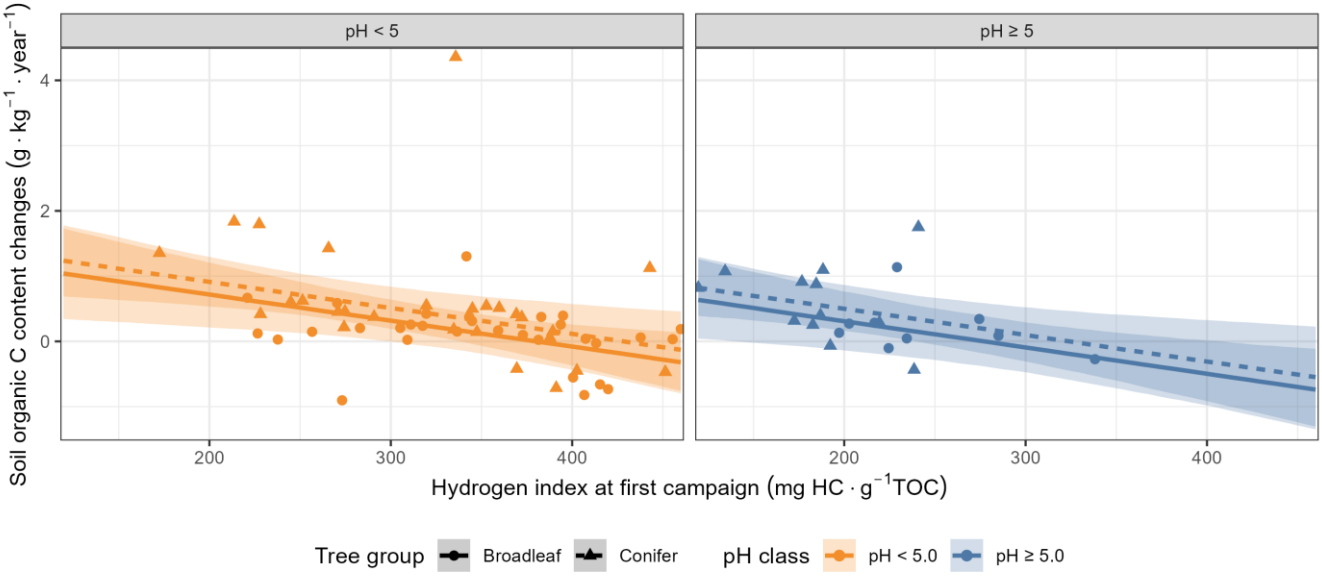


Figure 5: Model estimated effect of (a): forest floor C–stock variation, and (b): oxalate-extracted aluminium + 0.5 iron content on C–content changes for the 0–10 cm depth layer depending on pH class and tree functional group. The left panels are the relationships for the pH < 5 soils (orange), the right panels for pH ≥ 5 soils (blue). The broadleaf and coniferous stands are represented separately (solid lines and circles: broadleaf, dotted lines and triangles: conifer). The ribbons show the credible intervals at 95 % of the coefficients.

To be able to perform a comparison between the two model versions, the model without RE metrics has been redone without an observation which did not have a RE analysis at the first campaign (a *Q. petraea* site – CHS 35), though without

https://doi.org/10.5194/egusphere-2026-6489
Preprint. Discussion started: 9 November 2026
© Author(s) 2026. CC BY 4.0 License.

435 modification on the overall values of the parameters. The model with RE metrics was the best compared to the one without, with a Leave-One-Out Information Criterion of 146.6 and 151.7 respectively (Vehtari et al., 2017). The latter model was estimated to be worse than the former at 79 % using the method described by Sivula et al. (2025). However, this estimation might be biased as the number of observations was less than 100 (79).



440 **Figure 6: Model estimated effect of hydrogen index on C–content changes for the 0–10 cm depth layer depending on pH class and tree functional group. The left panels are the relationships for the pH < 5 soils (orange), the right panels for pH ≥ 5 soils (blue). The broadleaf and coniferous stands are represented separately (solid lines and circles: broadleaf, dotted lines and triangles: conifer). The ribbons show the credible intervals at 95 % of the coefficients.**

https://doi.org/10.5194/egusphere-2026-6489
Preprint. Discussion started: 9 November 2026
© Author(s) 2026. CC BY 4.0 License.

Table 5: Results of the models of annual variations of soil organic carbon content, hydrogen index and T_{50} CO_2 PYR for the 0–10 cm soil layer depth. The median coefficient values are shown, with the 95 % credible intervals in square brackets; the parameters different from 0 at 95 % credible intervals are in bold, and those different from 0 at 90 % are underlined. σ and ν are the other parameters estimated for the Student's t distribution. The variations are given in changes in g·kg soil^{-1}·year^{-1} for SOC, mg HC·g TOC^{-1}·year^{-1} for HI, and °C·year^{-1} for T_{50} CO_2 PYR.

	SOC content	SOC content (RE)	Hydrogen index	T_{50} CO_2 PYR
Intercept (broadleaf sites with pH ≥ 5)	0.01 [-0.38, 0.38]	-0.12 [-0.56, 0.32]	-0.89 [-2.15, 0.37]	-0.19 [-0.47, 0.09]
Functional group; Conifers	**0.45 [0.13, 0.79]**	0.20 [−0.16, 0.56]	-0.34 [-1.44, 0.78]	<u>-0.17 [-0.35, 0.02]</u>
Mean carbon content of both campaigns	-0.02 [-0.26, 0.22]	0.19 [−0.09, 0.48]		
Mean HI of both campaigns			-0.35 [-1.06, 0.36]	
Mean T_{50} CO_2 PYR of both campaigns				0.00 [-0.13, 0.14]
Regular litter	0.02 [-0.13, 0.17]	-0.04 [-0.18, 0.10]	-0.10 [-0.63, 0.38]	<u>-0.08 [-0.17, 0.01]</u>
Irregular litter	0.01 [-0.13, 0.16]	0.03 [-0.11, 0.18]	-0.14 [-0.58, 0.32]	0.02 [-0.06, 0.11]
Annual stock variation of the forest floor	**-0.19 [-0.35, -0.07]**	**-0.16 [-0.31, -0.04]**	**-0.67 [-1.10, -0.25]**	**0.11 [0.03, 0.18]**
Mean annual temperature	0.06 [-0.10, 0.21]	0.06 [−0.09, 0.21]	-0.11 [-0.65, 0.45]	0.01 [-0.10, 0.12]
Mean annual precipitation	-0.11 [-0.28, 0.08]	-0.07 [-0.22, 0.11]	-0.14 [-0.75, 0.47]	-0.01 [-0.11, 0.10]
Sites with pH < 5	0.12 [-0.30, 0.56]	0.43 [-0.12, 0.96]	0.23 [-1.33, 1.76]	0.09 [-0.28, 0.43]
Clay content; sites with pH ≥ 5	-0.05 [-0.29, 0.20]	-0.01 [-0.24, 0.23]	-0.20 [-0.98, 0.63]	-0.03 [-0.18, 0.12]
Clay content; sites with pH < 5	-0.04 [-0.35, 0.26]	-0.07 [-0.42, 0.24]	-0.07 [-1.10, 0.91]	0.12 [-0.08, 0.31]
Al_o + 0.5 Fe_o; sites with pH ≥ 5	<u>0.29 [-0.04, 0.65]</u>	0.04 [-0.38, 0.42]	0.42 [-0.59, 1.45]	0.09 [-0.12, 0.32]
Al_o + 0.5 Fe_o; sites with pH < 5	0.19 [-0.07, 0.46]	-0.11 [-0.45, 0.23]	0.34 [-0.48, 1.21]	-0.07 [-0.22, 0.07]
Ca^{2+} + Mg^{2+}; sites with pH ≥ 5	0.15 [-0.06, 0.35]	0.05 [-0.17, 0.26]	-0.24 [-0.87, 0.37]	0.04 [-0.08, 0.16]
Ca^{2+} + Mg^{2+}; sites with pH < 5	0.20 [-0.44, 0.88]	0.09 [-0.66, 0.82]	0.75 [-1.31, 2.78]	-0.02 [-0.47, 0.41]
T_{50} CO_2 PYR at first campaign		0.01 [-0.23, 0.25]		
Hydrogen index at first campaign		**-0.34 [-0.62, -0.07]**		
σ	0.39 [0.25, 0.55]	0.38 [0.26, 0.53]	1.54 [1.15, 1.92]	0.28 [0.23, 0.34]
ν	3.70 [1.58, 12.77]	4.02 [1.74, 13.46]	13.94 [3.28, 48.27]	20.93 [5.96, 61.68]

The hydrogen index decreased between the first and second campaign in each depth layer: -1.27 ± 1.84 mg HC·g TOC^{-1}·year^{-1} at 0–10 cm, -2.17 ± 2.06 at 10–20 cm, and -1.92 ± 2.66 at 20–40 cm, different from 0 at these three depths. The sole significant effect on HI was the negative effect of the forest floor C–stock variations (-0.67 [-1.10, -0.25]).

T_{50} CO_2 PYR decreased between the two campaigns only for the 0–10 cm layer, at -0.22 ± 0.30 °C·year^{-1}, compared to -0.03 ± 0.26 for the 10–20 cm layer, and -0.01 ± 0.29 for 20–40 cm. This was confirmed by the depth layer model, with a median decrease of -0.21 [-0.27, -0.15] °C·year^{-1}, against -0.05 [-0.11, 0.00] and -0.01 [-0.07, 0.05] for the two other layers. The C–stock variation of the forest floor also had an influence for this variable, positive this time (0.11 [0.03, 0.18]). Two other variables impacted T_{50} CO_2 PYR at 90%CI: the tree species functional group (a negative effect for the coniferous sites; -0.17 [90%CI -0.32, -0.01]), and the inputs of regular litter (-0.08 [90%CI -0.16, -0.01]).

https://doi.org/10.5194/egusphere-2026-6489
Preprint. Discussion started: 9 November 2026
© Author(s) 2026. CC BY 4.0 License.

4. Discussion

4.1 Determinants of soil organic carbon content

A shift in the drivers influencing SOC content was expected, as our first hypothesis (H1), from Al and Fe in organo-mineral complexes explaining SOC content at lower pH, to basic cations (Ca^{2+} + Mg^{2+}) and clay driving it at higher pH (Guidi et al., 2025; Rasmussen et al., 2018). However, we did not observe the expected shift in explanatory variables with pH (as summarised in Table 6). First off, we did not observe an effect of clay at high pH, contrary to what is assumed in most models of SOC dynamics, even if this lack of relationship between SOC and clay has already been described (Curtin et al., 2015; Fukumasu et al., 2021; von Fromm et al., 2021). For these high pH sites (pH ≥ 5), basic cations (Ca^{2+} and Mg^{2+}) increased SOC content at all depths. This positive effect of Ca^{2+} has already been found in multiple studies, reviewed by Rowley et al. (2018). However, we must be cautious about the potential bias arising from the fact that the organic matter may carry exchangeable basic cations. An accumulation of OM would therefore be responsible of an increase of base cations, and the accumulation of OM would not be a consequence of the higher cations content (Gruba and Mulder, 2015).

Oxalate-extracted metals also influenced SOC content at low but also at high pH. Nevertheless, the main influence of reactive metals on SOC in the RENECOFOR network was in accordance with current research, showing the importance of reactive metals in the stabilisation of SOC mainly between pH 5.5–6.5 (e.g. Heckman et al., 2023; Kleber et al., 2015; Rasmussen et al., 2018), and with the inclusion of SOC in Al and Fe oxides which may be observed up to pH 8 (Rowley et al., 2018). Few sites in our data set had high pH (six sites with pH > 6, and two with pH > 7) and it was therefore not possible to verify the effects only occurring in really high pH, where a lack of relationship between short-range ordered (SRO) minerals and SOC content was expected. More specifically, our results would fit into the organo-metallic "glue" hypothesis of Wagai et al. (2020). This hypothesis posits that organo-metal units act as a binding agent that promotes associations of organic molecules, metals and mineral particles such as clays, thereby forming microaggregates of meso-density (1.8 to 2.4 $g \cdot cm^{-3}$). But we observed that the link between SOC and oxalate-extractable metals applies to the bulk soil as a whole, regardless of aggregate density.

At pH ≥ 5, the positive effect of basic cations and oxalate-extracted metals were cumulative, suggesting that cations bridging could occur in poorly crystalline oxides, as observed at the subnanoscale by Van Der Kellen et al. (2022). von Fromm et al. (2021) also found a strong Ca^{2+} positive effect, additive with oxalate-extracted metals, even in acidic soils. But it was not the case for our sites, as there was no effect of basic cations for our pH < 5, representing the most acidic group of von Fromm et al. (2021).

Contrary to our second hypothesis (H2) under which we expected the effect of soil characteristics on SOC to increase with depth, the influence of soil properties was not particularly more pronounced as the layer became deeper. The effect of oxalate-extracted metals seemed to have a slightly larger positive effect on SOC for higher pH group sites in the deepest layers compared to 0–10 cm one, but the influence of oxalate-extracted metals and basic cations was of the same order of magnitude for the three studied layers. For other soil properties, their influence was higher in the topsoil, with a positive

https://doi.org/10.5194/egusphere-2026-6489
Preprint. Discussion started: 9 November 2026
© Author(s) 2026. CC BY 4.0 License.

effect at 90%CI of the lowest pH group and clay in this group in the 0–10 cm layer. However, since the concentration of C decreases with depth, the analytical sensitivity to detect a variation is limited, which could hinder the possibility to detect relationships. At the opposite of our hypothesis, some stand characteristics, irregular litter inputs and forest floor carbon stock, had a negative effect only in the deepest layer (20–40 cm), with no influence for more superficial layers. However, there were no plausible geo-chemical pathway to explain these relationships, and they were likely to be statistical artefacts. Nevertheless, coniferous stands showed a tendency to have a higher C–content in the 0–10 cm soil depth, which is an effect already described for SOC stocks in this network, without degraded sites exclusion of the dataset (Jonard et al., 2017), or for dual species comparisons (Osei et al., 2021; Osei et al., 2022). But the effect of functional group does not always occur (Schulp et al., 2008) and may be due to the local conditions: despite higher SOC content, some studies found no global effect between tree groups when several species were aggregated, with some broadleaf species having a comparable SOC stock to that of coniferous species (Oostra et al., 2006; Schulp et al., 2008). The aggregation of several species by group may therefore obscure more subtle effects from the species identity, but it would have made the estimation of the parameters' values challenging in our models given the number of sites per tree species.

In many predictive models of SOC dynamic, SOC is linearly related to C–inputs in a steady state regime, without considering a soil carbon saturation (Stewart et al., 2007), and its decomposition is generally increased by temperature (up to a tipping point) and precipitation or soil moisture (e.g. CENTURY Parton et al., 1987; Millennial Abramoff et al., 2022; Yasso Viskari et al., 2022). Therefore, the general lack of influence of temperature (except for 0–10 cm layer), precipitation, and litter inputs in our study was more surprising. In a meta-analysis, Feng et al. (2022) found an increase in C–inputs lead to a higher SOC stock or concentration, which was positively correlated with the litter input rate. However, this effect can be relatively small (Wrightson et al., 2025), or even not observable (Bowden et al., 2014). The lack of relationship between climatic variables and litter inputs in our study could also indicate that the majority of the sites were at steady state. This could also be explained by constraints affecting the decomposition processes, which may be mediated by the carbon compounds of SOM (Cotrufo et al., 2013), or by ecological limitations on microbial communities (Craig et al., 2021; Georgiou et al., 2017).

https://doi.org/10.5194/egusphere-2026-6489
Preprint. Discussion started: 9 November 2026
© Author(s) 2026. CC BY 4.0 License.

Table 6: Summary of models for SOC content, hydrogen index, T_{50} CO_2 PYR values at the second campaign, and the annual variations of SOC content, with the best model between the two SOC variation models being the SOC (RE), hydrogen index and T_{50} CO_2 PYR for the 0–10 cm soil layer. ↗ and ↘ stand for a positive and negative effect at 95 %; ↗ and ↘ stand for a positive and negative effect at 90 %.

	SOC content			Hydrogen Index			T_{50} CO_2 PYR			Variation (0–10 cm)			
	0–10	10–20	20–40	0–10	10–20	20–40	0–10	10–20	20–40	SOC (RE)	SOC	HI	T_{50} CO_2 PYR
Functional group; Conifers	↗	·	·	↘	↘	↘	·	·	·	·	↗	·	↘
Regular litter	·	·	·	↘	↘	·	·	·	·	·	·	·	↘
Irregular litter	·	·	↘	·	·	·	·	·	·	·	·	·	·
Mean annual temperature	↘	·	·	·	·	↗	·	·	·	·	·	·	·
Mean annual precipitation	·	·	·	·	·	↗	·	·	·	·	·	·	·
Sites with pH < 5	↗	↗	·	↗	↗	·	↘	↘	·	·	·	·	·
Clay content in sites with pH ≥ 5	·	·	·	·	·	·	·	·	·	·	·	·	·
Clay content in sites with pH < 5	↗	·	·	·	↘	↘	↗	↗	·	·	·	·	·
Al_o + 0.5 Fe_o in sites with pH ≥ 5	↗	↗	↗	·	·	↘	↗	↗	·	·	↗	·	·
Al_o + 0.5 Fe_o in sites with pH < 5	↗	↗	↗	↘	·	·	↗	↗	·	·	·	·	·
Ca^{2+} + Mg^{2+} in sites with pH ≥ 5	↗	↗	↗	·	·	↗	·	·	·	·	·	·	·
Ca^{2+} + Mg^{2+} in sites with pH < 5	·	·	·	·	↗	·	·	·	·	·	·	·	·
Forest floor carbon stock	·	·	↘	·	↗	·	·	·	·				
Average value of the two campaigns										·	·	·	·
Forest floor carbon stock variation										↘	↘	↘	↗
Hydrogen Index at first campaign										↘			
T_{50} CO_2 PYR at first campaign										·			

4.2 Factors influencing Rock-Eval® indices

We stated as our third hypothesis (H3) that HI would be primarily influenced by climate and stand characteristics, and that T_{50} CO_2 PYR would be mainly associated with soil properties. This hypothesis was partially confirmed. The Hydrogen Index, indicator of poorly decomposed OM, responded to a higher number of explanatory variables across all depths compared to T_{50} CO_2 PYR, indicative of SOC thermal stability. The lowest HI values for coniferous stands has already been observed for the POM in the 0–10 cm layer of a subset of RENECOFOR sites n = 52 (Soucémarianadin et al., 2019), and we are confirming this effect for the total SOC in a larger number of sites and for deeper soil layers. The negative effect of the litter inputs on HI was surprising, as we would have thought fresh litter would be of higher concentration of hydrocarbons, increasing the HI of the topsoil layer, but this effect appeared mainly due to the coniferous stands.

Contrary to our expectation, HI, representative of poorly decomposed C, was also explained by several soil properties for both pH groups. The negative effect of reactive metals on HI would indicate that associations of organic matter with SRO minerals are mainly formed with already decomposed carbon. From our analyses, this interaction depends on soil pH, with

https://doi.org/10.5194/egusphere-2026-6489
Preprint. Discussion started: 9 November 2026
© Author(s) 2026. CC BY 4.0 License.

this association occurring in the surface layer in low pH soil, and in deeper layers in higher pH. On the contrary, the positive effect of basic cations on HI for the 20–40 cm layer and pH ≥ 5 would indicate an association of clay with poorly decomposed SOM, which would be of plant origin (Saenger et al., 2013). Ca^{2+} and Mg^{2+} also had a positive effect on HI in sites with pH < 5 for the 10–20 cm layer. Ca–C relationship has already been observed in acidic soils (Rowley et al., 2023; Van Der Kellen et al., 2022) but in our results, this positive relationship seemed to be a spurious estimation of the model, as indicated by the wide credible interval for this relationship.

For the thermal stability of C, T_{50} CO_2 PYR, soil properties affected it solely for the 0–10 and 10–20 cm layers. Oxalate-extracted metals increased T_{50} CO_2 PYR for both pH groups, confirming the protecting role of SRO on SOM. This is in accordance with the higher proportion of oxidation resistant SOC with increasing Al_o content found by Fukumasu et al. (2021), and the negative effect of Fe_o on C mineralisation rate found by Huang et al. (2016). Clay content also increased T_{50} CO_2 PYR but only for the sites with pH < 5. This would confirm a relationship between pH and stable carbon proportion which has been observed by Yu et al. (2019) in forest soils whose pH was comparable with our lower pH group. This result would fit into the "glue" hypothesis, where more microbially-altered OM would be associated with clay particles (Wagai et al., 2020).

Soil pH had an important effect on RE parameters: T_{50} CO_2 PYR, SOC was lower in lower pH sites for the 0–10 and 10–20 cm layers, which was confirmed by the increase of HI. These results are in accordance with Delahaie et al. (2023), for whom pH had a negative effect on Rock-Eval® temperature parameters (including T_{50} CO_2 PYR), while clay content increased them. This reduced stability of OM in lower pH was not expected given that low pH favours inner-sphere complexation (Kleber et al., 2015), which is more stable than the other adsorption mechanisms (Sposito and Sposito, 2016). This may be due to the greater pH sensitivity of Al, which has a lower degree of precipitation with dissolved organic matter in low pH (Nierop et al., 2002). This effect of pH on the stability of OM has also been observed in alpine sites, with a greater proportion of weakly adsorbed carbon (from van der Waals interactions or outer-sphere complexation) in low pH (Niu et al., 2023).

4.3 Soil organic carbon content and Rock-Eval® indices variation

We stated as fourth hypothesis (H4) that variation in SOC content, hydrogen index, and T_{50} CO_2 PYR would be primarily affected by stand characteristics and climate rather than by soil properties. From our results, the variations between the two sampling campaigns of SOC content and T_{50} CO_2 PYR occurred mainly in the top layer (an average increase of 0.36 $g \cdot kg^{-1} \cdot year^{-1}$, and decrease of -0.22 $°C \cdot year^{-1}$ respectively), while a general decrease was observable in all layers for HI (-1.27, -2.17, and -1.92 mg $HC \cdot g\ TOC^{-1} \cdot year^{-1}$ for the 0–10, 10–20, and 20–40 cm layer respectively). The higher responsivity of the top layer can be explained by the age of its carbon, likely to be younger than the one of the deeper layers (Balesdent et al., 2018) and therefore would be more responsive than older carbon (Liebmann et al., 2020). However, SOC content, HI, and T_{50} CO_2 PYR variation were not explained by most of the included variables, thus leaving our fourth hypothesis

https://doi.org/10.5194/egusphere-2026-6489
Preprint. Discussion started: 9 November 2026
© Author(s) 2026. CC BY 4.0 License.

inconclusive, as we were unable to identify clear relationships between the variations and explanatory variables, notably stand characteristics and climate, as nearly all explanatory variables had no influence.

Only the SOC content variation was affected by one of the soil properties: the oxalate-extracted metals in high pH soils, even though at 90%CI, requiring further confirmation. This result shows the interactions between SOC and reactive minerals can occur in a relatively short time at the site level. This can confirm other results, such as Bruun et al. (2010) which found a reduced basal soil respiration in relationship with reactive minerals in tropical soils of the same pH range as the high pH group, or Dorau et al. (2019) who identified that sequestration of SOM by Fe oxides can be observed within 30 days experimentally. But based on other research on SOC mineralisation, we would have expected a positive effect of basic cations on SOC content variation, as Das et al. (2019) which found a negative effect of Ca^{2+} and Mg^{2+} on C mineralisation. Like has been observed for SOC content, we did not observe an effect of litter inputs for the C variation. This could either confirm the sites were in a steady state considering the average litter inputs, or, if not, a year-to-year change of carbon inputs on SOC cannot be identified over a 15–year interval. However, an absence of relationship between litter inputs and C–variation could also indicate high density-dependence of microbial communities, which could hinder short term variations of increased C–inputs (Georgiou et al., 2017).

Nevertheless, the nature of organic carbon allowed to better explain the variation in SOC content between the two campaigns. The first model showed an effect of the tree functional group, with more carbon being accumulated in coniferous stands compared to broadleaf, a trend already described by Jonard et al. (2017), along the limited effect of reactive metals content when pH ≥ 5. However, taking into account the Hydrogen Index of the first campaign allowed a better model, and showed that HI had a negative effect on the SOC variation, with an increase of SOC in lower values of HI to a decrease at highest hydrocarbon content. T_{50} CO_2 PYR had no impact, indicating that this metric does not seem relevant for changes at a decadal time frame. The effect of the tree group in the first model and the loss of this relationship when adding HI show the main effect of the tree group may arise from a different carbon composition of the carbon in these stands. This relationship was confirmed by the model of HI at the second campaign, which showed carbon in conifer stands had a lower HI, thus a more stable carbon. It would mean a lower decomposition speed allowed a higher accumulation in the soil (Mayer et al., 2020) for coniferous sites. However, contrary to previous assumptions, litter from coniferous species does not inherently decompose more slowly than that from broadleaf species (Augusto and Boča, 2022). The fact that many studies have shown a lower rate of decomposition in coniferous forests can be explained by more unfavourable local conditions in these stands (Albers et al., 2004; Berger and Berger, 2012). In our models, we integrated several climate and forest-related characteristics, however their selection or resolution may not be sufficient to identify these adverse effects. The decrease in decomposition rate may be due from non-described variables (e.g. polyphenol content – Gallet and Lebreton, 1995), which might be reflected in the hydrogen index of our second model.

Change in SOC content could also be explained by the transfer rate of carbon between the holorganic layer and the mineral soil. The negative relationship between the SOC content and the stock change of the forest floor would show that when more carbon was accumulated in the holorganic layers, less carbon was transferred to the lower layers. Some studies found a

https://doi.org/10.5194/egusphere-2026-6489
Preprint. Discussion started: 9 November 2026
© Author(s) 2026. CC BY 4.0 License.

disconnect between the O and mineral layers (Liebmann et al., 2020). For instance, an increase in aboveground litter inputs could only heighten the stock of the holorganic layer, while the mineral layers undergo only a minimal change, or even a decrease (Garten, 2009; Lajtha et al., 2014). This relationship has been recently observed on this dataset (Houballah et al., 2026) yet using a carbon dynamic modelling with a modification of the AMG model (Andriulo et al., 1999), allowing a forest floor compartment and a mineral soil compartment. However, the effects of the forest floor stock variation on the variations of SOC and RE indices can originate from differences in the sampling between the two campaigns regarding the identification of organic and mineral layers, where part of O or A layer could have been considered as the other one when the transition between the two layers could be difficult to distinguish, despite the operators' best efforts. As stated in the M&M, several sites were removed before the analyses in case of substantial perturbations (natural or from forest management), and when operators had specified that organic and mineral layers have been mixed. For the remaining stands, no observation from either campaign made us believe there was an important discrepancy in the sampling, but it was not possible to be unequivocal. If there had been a sampling difference, more upper mineral layer should have been considered as organic layer during the second campaign given the relationships between forest floor C–variation and SOC content, HI, and T_{50} CO_2 PYR of the 0–10 cm layer.

5. Conclusion

Contrary to previous research on the relationships between SOC and climate, stand and soil properties (e.g. Guidi et al., 2025; von Fromm et al., 2021), we investigated their effect not only on the SOC content, but also on other descriptors, via Rock-Eval® analysis, and on the annual variation of SOC content and RE parameters. We used a priori models, which allowed us to consider the effects the various included variables, and we expected a shift in explanatory variables given the soil pH. We identified already observed effects, such as the positive influence of reactive metals and basic cations on SOC content, but these two properties were not exclusive to each other in the studied forest sites and were even cumulative for highest pH soils. Furthermore, RE parameters gave more insights on the effect of soil properties on SOC. Thereby, reactive metals also increased stability of SOC, regardless of soil pH.

For the SOC content and RE parameters variation, few characteristics influenced them. The principal one was the variation of SOC in the holorganic layers, which could stem from a lower stabilisation in the mineral layer when more carbon is accumulated in the forest floor. For SOC content variation, we found the nature of SOC, through the HI, gave a better explanation than the functional tree group or soil properties.

A more surprising result was the lack of influence of some variables that are commonly used in models that predict SOC dynamics. Notably, mean annual temperature and precipitation in models control SOC decomposition, usually increasing mineralisation of carbon, and litter inputs are the main carbon source. Given this absence of effect, and the comparatively more important influence of soil characteristics on stability proxies of SOC, it would be crucial to better integrate soil properties in SOC dynamics models, beyond clay content which is included in some predictive models. Of the various

https://doi.org/10.5194/egusphere-2026-6489
Preprint. Discussion started: 9 November 2026
© Author(s) 2026. CC BY 4.0 License.

studied properties, reactive metals content is the most ubiquitous one, as it influenced SOC content, HI, T_{50} CO_2 PYR, and possibly SOC variation. However, these relationships should be verified in a wider network across a larger pH gradient. Furthermore, the nature of the SOC should be considered, given the important effect of HI on the SOC variation. Though, several models are already incorporating a variation in decomposition rate of different pools of carbon (e.g. Yasso – Viskari et al., 2022).

Data availability. The data used in the analyses and the R code are available at https://entrepot.recherche.data.gouv.fr/dataset.xhtml?persistentId=doi:10.57745/34ZTN6.

Author contribution. FM wrote the draft manuscript, performed the data analysis, and figure creation. DD and ZM co-directed this research from its initiation and edited the manuscript numerous times. PB and FB are the scientists that run the Rock-Eval® analyser and edited the manuscript, helped with data creation and analysis. MN is the scientist in charge of the RENECOFOR network and helped with the data analysis. LSA co-directed this research from its initiation and edited the manuscript numerous times.

Competing interests. The contact author has declared that none of the authors has any competing interests.

Acknowledgements. We thank the Office National des Forêts (National Forests Office), in charge of the RENECOFOR network, and specifically Sébastien Macé for providing us the RENECOFOR data. We thank the Météo-France administration which collected the climate data, as well as all people who contributed to the data acquisition.

Financial support. This research has been funded by the ANR FISSA project (ANR-21-CE32-0010) and by the ALAMOD project (ANR-22-PEXF-0002). They are respectively a research grant funded by the Agence Nationale de la Recherche (ANR – French National Research Agency) under the 2021 Generic Call for Proposals (AAPG2021), and a targeted research contract funded by the ANR as part of the exploratory PEPR FairCarboN program.

6. References

Abramoff, R., Xu, X., Hartman, M., O'Brien, S., Feng, W., Davidson, E., Finzi, A., Moorhead, D., Schimel, J., Torn, M., and Mayes, M. A.: The Millennial model: In search of measurable pools and transformations for modeling soil carbon in the new century, Biogeochemistry, 137, 51–71, https://doi.org/10.1007/s10533-017-0409-7, 2018.

Abramoff, R. Z., Guenet, B., Zhang, H., Georgiou, K., Xu, X., Viscarra Rossel, R. A., Yuan, W., and Ciais, P.: Improved global-scale predictions of soil carbon stocks with Millennial Version 2, Soil Biology and Biochemistry, 164, 108466, https://doi.org/10.1016/j.soilbio.2021.108466, 2022.

Albers, D., Migge, S., Schaefer, M., and Scheu, S.: Decomposition of beech leaves (*Fagus Sylvatica*) and spruce needles (*Picea Abies*) in pure and mixed stands of beech and spruce, Soil Biology and Biochemistry, 36, 155–164, https://doi.org/10.1016/j.soilbio.2003.09.002, 2004.

Andriulo, A., Mary, B., and Guerif, J.: Modelling soil carbon dynamics with various cropping sequences on the rolling pampas, Agronomie, 19, 365–377, https://doi.org/10.1051/agro:19990504, 1999.

https://doi.org/10.5194/egusphere-2026-6489
Preprint. Discussion started: 9 November 2026
© Author(s) 2026. CC BY 4.0 License.

Anne, P.: Sur le dosage rapide du carbone organique dans le sol, Annales d'Agronomie, 2, 162–172, 1945.

Augusto, L. and Boča, A.: Tree functional traits, forest biomass, and tree species diversity interact with site properties to drive forest soil carbon, Nature Communications, 13, 1097, https://doi.org/10.1038/s41467-022-28748-0, 2022.

Baldocchi, D., Chu, H., and Reichstein, M.: Inter-annual variability of net and gross ecosystem carbon fluxes: A review, Agricultural and Forest Meteorology, 249, 520–533, https://doi.org/10.1016/j.agrformet.2017.05.015, 2018.

Balesdent, J., Basile-Doelsch, I., Chadoeuf, J., Cornu, S., Derrien, D., Fekiacova, Z., and Hatté, C.: Atmosphere–soil carbon transfer as a function of soil depth, Nature, 559, 599–602, https://doi.org/10.1038/s41586-018-0328-3, 2018.

Barré, P., Fernandez-Ugalde, O., Virto, I., Velde, B., and Chenu, C.: Impact of phyllosilicate mineralogy on organic carbon stabilization in soils: Incomplete knowledge and exciting prospects, Geoderma, 235–236, 382–395, https://doi.org/10.1016/j.geoderma.2014.07.029, 2014.

Barré, P., Cécillon, L., and Kanari, E.: Characterization and Evaluation of the Stability of Soil Organic Matter, in: The Rock-Eval Method, John Wiley & Sons, Ltd, 181–207, https://doi.org/10.1002/9781394256235.ch10, 2024.

Baudin, F., Disnar, J.-R., Aboussou, A., and Savignac, F.: Guidelines for Rock–Eval analysis of recent marine sediments, Organic Geochemistry, 86, 71–80, https://doi.org/10.1016/j.orggeochem.2015.06.009, 2015.

Behar, F., Beaumont, V., and Penteado, H. L. D. B.: Rock-Eval 6 Technology: Performances and Developments, Oil & Gas Science and Technology, 56, 111–134, https://doi.org/10.2516/ogst:2001013, 2001.

Beillouin, D., Corbeels, M., Demenois, J., Berre, D., Boyer, A., Fallot, A., Feder, F., and Cardinael, R.: A global meta-analysis of soil organic carbon in the Anthropocene, Nature Communications, 14, 3700, https://doi.org/10.1038/s41467-023-39338-z, 2023.

Berger, T. W. and Berger, P.: Greater accumulation of litter in spruce (Picea abies) compared to beech (Fagus sylvatica) stands is not a consequence of the inherent recalcitrance of needles, Plant and Soil, 358, 349–369, https://doi.org/10.1007/s11104-012-1165-z, 2012.

Bölscher, T., Cardon, Z. G., Garcia Arredondo, M., Grand, S., Griffen, G., Hestrin, R., Imboden, J., Jamoteau, F., Lacroix, E. M., Pérez Castro, S., Persson, P., Riley, W. J., and Keiluweit, M.: Vulnerability of mineral-organic associations in the rhizosphere, Nature Communications, 16, 5527, https://doi.org/10.1038/s41467-025-61273-4, 2025.

Bowden, R. D., Deem, L., Plante, A. F., Peltre, C., Nadelhoffer, K., and Lajtha, K.: Litter Input Controls on Soil Carbon in a Temperate Deciduous Forest, Soil Science Society of America Journal, 78, S66–S75, https://doi.org/10.2136/sssaj2013.09.0413nafsc, 2014.

Bramble, D. S. E., Ulrich, S., Schöning, I., Mikutta, R., Brandt, L., Poll, C., Kandeler, E., Mikutta, C., Konrad, A., Siemens, J., Yang, Y., Polle, A., Schall, P., Ammer, C., Kaiser, K., and Schrumpf, M.: Formation of mineral-associated organic matter in temperate soils is primarily controlled by mineral type and modified by land use and management intensity, Global Change Biology, 30, e17024, https://doi.org/10.1111/gcb.17024, 2024.

Brêthes, A., Brun, J.-J., Jabiol, B., Ponge, J.-F., and Toutain, F.: Classification of forest humus forms: A French proposal, Annales des sciences forestières, 52, 535–546, https://doi.org/10.1051/forest:19950602, 1995.

https://doi.org/10.5194/egusphere-2026-6489
Preprint. Discussion started: 9 November 2026
© Author(s) 2026. CC BY 4.0 License.

Bruun, T. B., Elberling, B., and Christensen, B. T.: Lability of soil organic carbon in tropical soils with different clay minerals, Soil Biology and Biochemistry, 42, 888–895, https://doi.org/10.1016/j.soilbio.2010.01.009, 2010.

Bürkner, P.-C.: Brms: An R Package for Bayesian Multilevel Models Using Stan, Journal of Statistical Software, 80, https://doi.org/10.18637/jss.v080.i01, 2017.

Cairns, M. A., Brown, S., Helmer, E. H., and Baumgardner, G. A.: Root biomass allocation in the world's upland forests, Oecologia, 111, 1–11, https://doi.org/10.1007/s004420050201, 1997.

Cécillon, L., Baudin, F., Chenu, C., Christensen, B. T., Franko, U., Houot, S., Kanari, E., Kätterer, T., Merbach, I., van Oort, F., Poeplau, C., Quezada, J. C., Savignac, F., Soucémarianadin, L. N., and Barré, P.: Partitioning soil organic carbon into its centennially stable and active fractions with machine-learning models based on Rock-Eval® thermal analysis (PARTY$_{SOC}$v2.0 and PARTY$_{SOC}$v2.0$_{EU}$), Geoscientific Model Development, 14, 3879–3898, https://doi.org/10.5194/gmd-14-3879-2021, 2021.

Chen, X., Taylor, A. R., Reich, P. B., Hisano, M., Chen, H. Y. H., and Chang, S. X.: Tree diversity increases decadal forest soil carbon and nitrogen accrual, Nature, 618, 94–101, https://doi.org/10.1038/s41586-023-05941-9, 2023.

Coleman, K., Prout, J. M., and Milne, A. E.: RothC - A model for the turnover of carbon in soil, 2024.

Cotrufo, M. F., Wallenstein, M. D., Boot, C. M., Denef, K., and Paul, E.: The Microbial Efficiency-Matrix Stabilization (MEMS) framework integrates plant litter decomposition with soil organic matter stabilization: Do labile plant inputs form stable soil organic matter?, Global Change Biology, 19, 988–995, https://doi.org/10.1111/gcb.12113, 2013.

Craig, M. E., Mayes, M. A., Sulman, B. N., and Walker, A. P.: Biological mechanisms may contribute to soil carbon saturation patterns, Global Change Biology, 27, 2633–2644, https://doi.org/10.1111/gcb.15584, 2021.

Curtin, D., Beare, M. H., and Qiu, W.: Texture effects on carbon stabilisation and storage in New Zealand soils containing predominantly 2 : 1 clays, Soil Research, 54, 30–37, https://doi.org/10.1071/SR14292, 2015.

Das, S., Richards, B. K., Hanley, K. L., Krounbi, L., Walter, M. F., Walter, M. T., Steenhuis, T. S., and Lehmann, J.: Lower mineralizability of soil carbon with higher legacy soil moisture, Soil Biology and Biochemistry, 130, 94–104, https://doi.org/10.1016/j.soilbio.2018.12.006, 2019.

Dawud, S. M., Raulund-Rasmussen, K., Domisch, T., Finér, L., Jaroszewicz, B., and Vesterdal, L.: Is Tree Species Diversity or Species Identity the More Important Driver of Soil Carbon Stocks, C/N Ratio, and pH?, Ecosystems, 19, 645–660, https://doi.org/10.1007/s10021-016-9958-1, 2016.

Delahaie, A. A., Barré, P., Baudin, F., Arrouays, D., Bispo, A., Boulonne, L., Chenu, C., Jolivet, C., Martin, M. P., Ratié, C., Saby, N. P. A., Savignac, F., and Cécillon, L.: Elemental stoichiometry and Rock-Eval® thermal stability of organic matter in French topsoils, SOIL, 9, 209–229, https://doi.org/10.5194/soil-9-209-2023, 2023.

Desie, E., Muys, B., Jansen, B., Vesterdal, L., and Vancampenhout, K.: Pedogenic Threshold in Acidity Explains Context-Dependent Tree Species Effects on Soil Carbon, Frontiers in Forests and Global Change, 4, https://doi.org/10.3389/ffgc.2021.679813, 2021.

https://doi.org/10.5194/egusphere-2026-6489
Preprint. Discussion started: 9 November 2026
© Author(s) 2026. CC BY 4.0 License.

Dignac, M.-F., Derrien, D., Barré, P., Barot, S., Cécillon, L., Chenu, C., Chevallier, T., Freschet, G. T., Garnier, P., Guenet, B., Hedde, M., Klumpp, K., Lashermes, G., Maron, P.-A., Nunan, N., Roumet, C., and Basile-Doelsch, I.: Increasing soil carbon storage: Mechanisms, effects of agricultural practices and proxies. A review, Agronomy for Sustainable Development, 37, 14, https://doi.org/10.1007/s13593-017-0421-2, 2017.

Disnar, J. R., Guillet, B., Keravis, D., Di-Giovanni, C., and Sebag, D.: Soil organic matter (SOM) characterization by Rock-Eval pyrolysis: Scope and limitations, Organic Geochemistry, 34, 327–343, https://doi.org/10.1016/S0146-6380(02)00239-5, 2003.

Dorau, K., Pohl, L., Just, C., Höschen, C., Ufer, K., Mansfeldt, T., and Mueller, C. W.: Soil Organic Matter and Phosphate Sorption on Natural and Synthetic Fe Oxides under in Situ Conditions, Environmental Science & Technology, 53, 13081–13087, https://doi.org/10.1021/acs.est.9b03260, 2019.

Dunn, P. K. and Smyth, G. K.: Randomized Quantile Residuals, Journal of Computational and Graphical Statistics, 5, 236–244, https://doi.org/10.2307/1390802, 1996.

Feng, J., He, K., Zhang, Q., Han, M., and Zhu, B.: Changes in plant inputs alter soil carbon and microbial communities in forest ecosystems, Global Change Biology, 28, 3426–3440, https://doi.org/10.1111/gcb.16107, 2022.

Friedlingstein, P., O'Sullivan, M., Jones, M. W., Andrew, R. M., Hauck, J., Landschützer, P., Le Quéré, C., Li, H., Luijkx, I. T., Olsen, A., Peters, G. P., Peters, W., Pongratz, J., Schwingshackl, C., Sitch, S., Canadell, J. G., Ciais, P., Jackson, R. B., Alin, S. R., Arneth, A., Arora, V., Bates, N. R., Becker, M., Bellouin, N., Berghoff, C. F., Bittig, H. C., Bopp, L., Cadule, P., Campbell, K., Chamberlain, M. A., Chandra, N., Chevallier, F., Chini, L. P., Colligan, T., Decayeux, J., Djeutchouang, L. M., Dou, X., Duran Rojas, C., Enyo, K., Evans, W., Fay, A. R., Feely, R. A., Ford, D. J., Foster, A., Gasser, T., Gehlen, M., Gkritzalis, T., Grassi, G., Gregor, L., Gruber, N., Gürses, Ö., Harris, I., Hefner, M., Heinke, J., Hurtt, G. C., Iida, Y., Ilyina, T., Jacobson, A. R., Jain, A. K., Jarníková, T., Jersild, A., Jiang, F., Jin, Z., Kato, E., Keeling, R. F., Klein Goldewijk, K., Knauer, J., Korsbakken, J. I., Lan, X., Lauvset, S. K., Lefèvre, N., Liu, Z., Liu, J., Ma, L., Maksyutov, S., Marland, G., Mayot, N., McGuire, P. C., Metzl, N., Monacci, N. M., Morgan, E. J., Nakaoka, S.-I., Neill, C., Niwa, Y., Nützel, T., Olivier, L., Ono, T., Palmer, P. I., Pierrot, D., Qin, Z., Resplandy, L., Roobaert, A., Rosan, T. M., Rödenbeck, C., Schwinger, J., Smallman, T. L., Smith, S. M., Sospedra-Alfonso, R., Steinhoff, T., et al.: Global Carbon Budget 2024, Earth System Science Data, 17, 965–1039, https://doi.org/10.5194/essd-17-965-2025, 2025.

Fukumasu, J., Poeplau, C., Coucheney, E., Jarvis, N., Klöffel, T., Koestel, J., Kätterer, T., Nimblad Svensson, D., Wetterlind, J., and Larsbo, M.: Oxalate-extractable aluminum alongside carbon inputs may be a major determinant for organic carbon content in agricultural topsoils in humid continental climate, Geoderma, 402, 115345, https://doi.org/10.1016/j.geoderma.2021.115345, 2021.

Gabry, J., Češnovar, R., Johnson, A., and Bronder, S.: Cmdstanr: R Interface to 'CmdStan', 2025.

Gallet, C. and Lebreton, P.: Evolution of phenolic patterns in plants and associated litters and humus of a mountain forest ecosystem, Soil Biology and Biochemistry, 27, 157–165, https://doi.org/10.1016/0038-0717(94)00167-Y, 1995.

https://doi.org/10.5194/egusphere-2026-6489
Preprint. Discussion started: 9 November 2026
© Author(s) 2026. CC BY 4.0 License.

Garten, C. T.: A disconnect between O horizon and mineral soil carbon – Implications for soil C sequestration, Acta Oecologica, 35, 218–226, https://doi.org/10.1016/j.actao.2008.10.004, 2009.

Georgiou, K., Abramoff, R. Z., Harte, J., Riley, W. J., and Torn, M. S.: Microbial community-level regulation explains soil carbon responses to long-term litter manipulations, Nature Communications, 8, 1223, https://doi.org/10.1038/s41467-017-01116-z, 2017.

Gruba, P. and Mulder, J.: Tree species affect cation exchange capacity (CEC) and cation binding properties of organic matter in acid forest soils, Science of The Total Environment, 511, 655–662, https://doi.org/10.1016/j.scitotenv.2015.01.013, 2015.

Guidi, C., Gosheva-Oney, S., Didion, M., Flury, R., Walthert, L., Zimmermann, S., Oney, B. J., Niklaus, P. A., Thürig, E., Viskari, T., Liski, J., and Hagedorn, F.: Drivers of soil organic carbon from temperate to alpine forests: A model-based analysis of the Swiss forest soil inventory with Yasso20, Biogeosciences, 22, 4107–4122, https://doi.org/10.5194/bg-22-4107-2025, 2025.

Hall, S. J. and Thompson, A.: What do relationships between extractable metals and soil organic carbon concentrations mean?, Soil Science Society of America Journal, 86, 195–208, https://doi.org/10.1002/saj2.20343, 2022.

Harris, D., Horwáth, W. R., and van Kessel, C.: Acid fumigation of soils to remove carbonates prior to total organic carbon or CARBON-13 isotopic analysis, Soil Science Society of America Journal, 65, 1853–1856, https://doi.org/10.2136/sssaj2001.1853, 2001.

Hartig, F.: DHARMa: Residual Diagnostics for Hierarchical (Multi-Level / Mixed) Regression Models, https://doi.org/10.32614/CRAN.package.DHARMa, 2026.

Hassink, J.: The capacity of soils to preserve organic C and N by their association with clay and silt particles, Plant and Soil, 191, 77–87, https://doi.org/10.1023/A:1004213929699, 1997.

Heckman, K. A., Possinger, A. R., Badgley, B. D., Bowman, M. M., Gallo, A. C., Hatten, J. A., Nave, L. E., SanClements, M. D., Swanston, C. W., Weiglein, T. L., Wieder, W. R., and Strahm, B. D.: Moisture-driven divergence in mineral-associated soil carbon persistence, Proceedings of the National Academy of Sciences, 120, e2210044120, https://doi.org/10.1073/pnas.2210044120, 2023.

Hoffman, M. D. and Gelman, A.: The No-U-Turn Sampler: Adaptively Setting Path Lengths in Hamiltonian Monte Carlo, Journal of Machine Learning Research, 15, 2014.

Houballah, M., Clivot, H., Ferchaud, F., Noë, J. L., Barré, P., Cécillon, L., Guenet, B., Nicolas, M., Bruni, E., Paris, J.-M., Baudin, F., and Delpierre, N.: Simulation of decadal variations in soil organic carbon stocks in French forests, Geoderma, 472, 117926, https://doi.org/10.1016/j.geoderma.2026.117926, 2026.

Huang, X., Jiang, H., Li, Y., Ma, Y., Tang, H., Ran, W., and Shen, Q.: The role of poorly crystalline iron oxides in the stability of soil aggregate-associated organic carbon in a rice–wheat cropping system, Geoderma, 279, 1–10, https://doi.org/10.1016/j.geoderma.2016.05.011, 2016.

Ito, A. and Wagai, R.: Global distribution of clay-size minerals on land surface for biogeochemical and climatological studies, Scientific Data, 4, 170103, https://doi.org/10.1038/sdata.2017.103, 2017.

https://doi.org/10.5194/egusphere-2026-6489
Preprint. Discussion started: 9 November 2026
© Author(s) 2026. CC BY 4.0 License.

IUSS Working Group WRB: World Reference Base for Soil Resources. International soil classification system for naming soils and creating legends for soil maps, 4th edition., International Union of Soil Sciences, Vienna, Austria, 2022.

Jobbágy, E. G. and Jackson, R. B.: The Vertical Distribution of Soil Organic Carbon and Its Relation to Climate and Vegetation, Ecological Applications, 10, 423–436, https://doi.org/10.1890/1051-0761(2000)010[0423:TVDOSO]2.0.CO;2, 2000.

Jonard, M., Nicolas, M., Coomes, D. A., Caignet, I., Saenger, A., and Ponette, Q.: Forest soils in France are sequestering substantial amounts of carbon, Science of The Total Environment, 574, 616–628, https://doi.org/10.1016/j.scitotenv.2016.09.028, 2017.

Karhu, K., Fritze, H., Hämäläinen, K., Vanhala, P., Jungner, H., Oinonen, M., Sonninen, E., Tuomi, M., Spetz, P., Kitunen, V., and Liski, J.: Temperature sensitivity of soil carbon fractions in boreal forest soil, Ecology, 91, 370–376, https://doi.org/10.1890/09-0478.1, 2010.

Kleber, M., Mikutta, R., Torn, M. S., and Jahn, R.: Poorly crystalline mineral phases protect organic matter in acid subsoil horizons, European Journal of Soil Science, 56, 717–725, https://doi.org/10.1111/j.1365-2389.2005.00706.x, 2005.

Kleber, M., Eusterhues, K., Keiluweit, M., Mikutta, C., Mikutta, R., and Nico, P. S.: Chapter One - Mineral–Organic Associations: Formation, Properties, and Relevance in Soil Environments, in: Advances in Agronomy, vol. 130, edited by: Sparks, D. L., Academic Press, 1–140, https://doi.org/10.1016/bs.agron.2014.10.005, 2015.

Kleber, M., Bourg, I. C., Coward, E. K., Hansel, C. M., Myneni, S. C. B., and Nunan, N.: Dynamic interactions at the mineral–organic matter interface, Nature Reviews Earth & Environment, 2, 402–421, https://doi.org/10.1038/s43017-021-00162-y, 2021.

Lajtha, K., Bowden, R. D., and Nadelhoffer, K.: Litter and Root Manipulations Provide Insights into Soil Organic Matter Dynamics and Stability, Soil Science Society of America Journal, 78, S261–S269, https://doi.org/10.2136/sssaj2013.08.0370nafsc, 2014.

Lavallee, J. M., Soong, J. L., and Cotrufo, M. F.: Conceptualizing soil organic matter into particulate and mineral-associated forms to address global change in the 21st century, Global Change Biology, 26, 261–273, https://doi.org/10.1111/gcb.14859, 2020.

Liebmann, P., Wordell-Dietrich, P., Kalbitz, K., Mikutta, R., Kalks, F., Don, A., Woche, S. K., Dsilva, L. R., and Guggenberger, G.: Relevance of aboveground litter for soil organic matter formation – a soil profile perspective, Biogeosciences, 17, 3099–3113, https://doi.org/10.5194/bg-17-3099-2020, 2020.

Liski, J., Nissinen, A., Erhard, M., and Taskinen, O.: Climatic effects on litter decomposition from arctic tundra to tropical rainforest, Global Change Biology, 9, 575–584, https://doi.org/10.1046/j.1365-2486.2003.00605.x, 2003.

Lugato, E., Lavallee, J. M., Haddix, M. L., Panagos, P., and Cotrufo, M. F.: Different climate sensitivity of particulate and mineral-associated soil organic matter, Nature Geoscience, 14, 295–300, https://doi.org/10.1038/s41561-021-00744-x, 2021.

https://doi.org/10.5194/egusphere-2026-6489
Preprint. Discussion started: 9 November 2026
© Author(s) 2026. CC BY 4.0 License.

Mao, Z., Derrien, D., Didion, M., Liski, J., Eglin, T., Nicolas, M., Jonard, M., and Saint-André, L.: Modeling soil organic carbon dynamics in temperate forests with Yasso07, Biogeosciences, 16, 1955–1973, https://doi.org/10.5194/bg-16-1955-2019, 2019.

Mathieu, J. A., Hatté, C., Balesdent, J., and Parent, É.: Deep soil carbon dynamics are driven more by soil type than by climate: A worldwide meta-analysis of radiocarbon profiles, Global Change Biology, 21, 4278–4292, https://doi.org/10.1111/gcb.13012, 2015.

Mayer, M., Prescott, C. E., Abaker, W. E. A., Augusto, L., Cécillon, L., Ferreira, G. W. D., James, J., Jandl, R., Katzensteiner, K., Laclau, J.-P., Laganière, J., Nouvellon, Y., Paré, D., Stanturf, J. A., Vanguelova, E. I., and Vesterdal, L.: Tamm Review: Influence of forest management activities on soil organic carbon stocks: A knowledge synthesis, Forest Ecology and Management, 466, 118127, https://doi.org/10.1016/j.foreco.2020.118127, 2020.

Mayer, M., Rusch, S., Didion, M., Baltensweiler, A., Walthert, L., Ranft, F., Rigling, A., Zimmermann, S., and Hagedorn, F.: Elevation dependent response of soil organic carbon stocks to forest windthrow, Science of The Total Environment, 857, 159694, https://doi.org/10.1016/j.scitotenv.2022.159694, 2023.

McElreath, R.: Statistical rethinking: A Bayesian course with examples in R and Stan, Second edition., CRC Press, Boca Raton, 2020.

NF ISO 10390: Soil quality – determination of pH, 2004.

NF ISO 10694: Soil quality – determination of organic and total carbon after dry combustion (elementary analysis), 1995.

NF ISO 11260: Soil quality – determination of effective cation exchange capacity and base saturation level using barium chloride solution, 1994.

NF ISO 22036: Soil quality – Determination of trace elements in extracts of soil by inductively coupled plasma - atomic emission spectrometry (ICP - AES), 2009.

NF X 31-107: Soil Quality – Particle Size Determination by Sedimentation – Pipette Method, 2003.

NF X31-109: Soil quality – chemical methods – determination of organic carbon by sulfochromic oxidation, 1993.

Nierop, K. G. J., Jansen, B., and Verstraten, J. M.: Dissolved organic matter, aluminium and iron interactions: Precipitation induced by metal/carbon ratio, pH and competition, The Science of the Total Environment, 300, 201–211, https://doi.org/10.1016/s0048-9697(02)00254-1, 2002.

Niu, B., Lei, T., Chen, Q., Shao, M., Yang, X., Jiao, H., Yang, Y., Guggenberger, G., and Zhang, G.: pH: A core node of interaction networks among soil organo-mineral fractions, Environment International, 178, 108058, https://doi.org/10.1016/j.envint.2023.108058, 2023.

Oldham, P. D.: A note on the analysis of repeated measurements of the same subjects, Journal of Chronic Diseases, 15, 969–977, https://doi.org/10.1016/0021-9681(62)90116-9, 1962.

Oostra, S., Majdi, H., and Olsson, M.: Impact of tree species on soil carbon stocks and soil acidity in southern Sweden, Scandinavian Journal of Forest Research, 21, 364–371, https://doi.org/10.1080/02827580600950172, 2006.

https://doi.org/10.5194/egusphere-2026-6489
Preprint. Discussion started: 9 November 2026
© Author(s) 2026. CC BY 4.0 License.

Osei, R., Titeux, H., Bielak, K., Bravo, F., Collet, C., Cools, C., Cornelis, J.-T., Heym, M., Korboulewsky, N., Löf, M., Muys, B., Najib, Y., Nothdurft, A., Pach, M., Pretzsch, H., del Rio, M., Ruiz-Peinado, R., and Ponette, Q.: Tree species identity drives soil organic carbon storage more than species mixing in major two-species mixtures (pine, oak, beech) in Europe, Forest Ecology and Management, 481, 118752, https://doi.org/10.1016/j.foreco.2020.118752, 2021.

Osei, R., del Río, M., Ruiz-Peinado, R., Titeux, H., Bielak, K., Bravo, F., Collet, C., Cools, C., Cornelis, J.-T., Drössler, L., Heym, M., Korboulewsky, N., Löf, M., Muys, B., Najib, Y., Nothdurft, A., Pretzsch, H., Skrzyszewski, J., and Ponette, Q.: The distribution of carbon stocks between tree woody biomass and soil differs between Scots pine and broadleaved species (beech, oak) in European forests, European Journal of Forest Research, 141, 467–480, https://doi.org/10.1007/s10342-022-01453-9, 2022.

Osman, K. T.: Forest Soils, Springer International Publishing, Cham, https://doi.org/10.1007/978-3-319-02541-4, 2013.

Ouimette, A. P., Ollinger, S. V., Lepine, L. C., Stephens, R. B., Rowe, R. J., Vadeboncoeur, M. A., Tumber-Davila, S. J., and Hobbie, E. A.: Accounting for Carbon Flux to Mycorrhizal Fungi May Resolve Discrepancies in Forest Carbon Budgets, Ecosystems, 23, 715–729, https://doi.org/10.1007/s10021-019-00440-3, 2020.

Pacini, L., Adatte, T., Barré, P., Boussafir, M., Bouton, N., Cécillon, L., Lamoureux-Var, V., Sebag, D., Verrecchia, E., Wattripont, A., and Baudin, F.: Reproducibility of Rock-Eval® thermal analysis for soil organic matter characterization, Organic Geochemistry, 186, 104687, https://doi.org/10.1016/j.orggeochem.2023.104687, 2023.

Parton, W. J., Schimel, D. S., Cole, C. V., and Ojima, D. S.: Analysis of Factors Controlling Soil Organic Matter Levels in Great Plains Grasslands, Soil Science Society of America Journal, 51, 1173–1179, https://doi.org/10.2136/sssaj1987.03615995005100050015x, 1987.

Posit team: RStudio: Integrated Development Environment for R, 2025.

R Core Team: R: A language and environment for statistical computing, 2025.

Rasmussen, C., Heckman, K., Wieder, W. R., Keiluweit, M., Lawrence, C. R., Berhe, A. A., Blankinship, J. C., Crow, S. E., Druhan, J. L., Hicks Pries, C. E., Marin-Spiotta, E., Plante, A. F., Schädel, C., Schimel, J. P., Sierra, C. A., Thompson, A., and Wagai, R.: Beyond clay: Towards an improved set of variables for predicting soil organic matter content, Biogeochemistry, 137, 297–306, https://doi.org/10.1007/s10533-018-0424-3, 2018.

Reichenbach, M., Fiener, P., Garland, G., Griepentrog, M., Six, J., and Doetterl, S.: The role of geochemistry in organic carbon stabilization against microbial decomposition in tropical rainforest soils, SOIL, 7, 453–475, https://doi.org/10.5194/soil-7-453-2021, 2021.

Rowley, M. C., Grand, S., and Verrecchia, É. P.: Calcium-mediated stabilisation of soil organic carbon, Biogeochemistry, 137, 27–49, https://doi.org/10.1007/s10533-017-0410-1, 2018.

Rowley, M. C., Nico, P. S., Bone, S. E., Marcus, M. A., Pegoraro, E. F., Castanha, C., Kang, K., Bhattacharyya, A., Torn, M. S., and Peña, J.: Association between soil organic carbon and calcium in acidic grassland soils from Point Reyes National Seashore, CA, Biogeochemistry, 165, 91–111, https://doi.org/10.1007/s10533-023-01059-2, 2023.

https://doi.org/10.5194/egusphere-2026-6489
Preprint. Discussion started: 9 November 2026
© Author(s) 2026. CC BY 4.0 License.

Saenger, A., Cécillon, L., Sebag, D., and Brun, J.-J.: Soil organic carbon quantity, chemistry and thermal stability in a mountainous landscape: A Rock–Eval pyrolysis survey, Organic Geochemistry, 54, 101–114, https://doi.org/10.1016/j.orggeochem.2012.10.008, 2013.

Schiedung, M., Barré, P., and Peoplau, C.: Separating fast from slow cycling soil organic carbon – A multi-method comparison on land use change sites, Geoderma, 453, 117154, https://doi.org/10.1016/j.geoderma.2024.117154, 2025.

Schulp, C. J. E., Nabuurs, G.-J., Verburg, P. H., and de Waal, R. W.: Effect of tree species on carbon stocks in forest floor and mineral soil and implications for soil carbon inventories, Forest Ecology and Management, 256, 482–490, https://doi.org/10.1016/j.foreco.2008.05.007, 2008.

Schulten, H.-R. and Leinweber, P.: Influence of the mineral matrix on the formation and molecular composition of soil organic matter in a long-term, agricultural experiment, Biogeochemistry, 22, 1–22, https://doi.org/10.1007/BF00002754, 1993.

Sivula, T., Magnusson, M., Matamoros, A. A., and Vehtari, A.: Uncertainty in Bayesian Leave-One-Out Cross-Validation Based Model Comparison, Bayesian Analysis, 1–31, https://doi.org/10.1214/25-BA1569, 2025.

Soucémarianadin, L., Cécillon, L., Chenu, C., Baudin, F., Nicolas, M., Girardin, C., Delahaie, A., and Barré, P.: Heterogeneity of the chemical composition and thermal stability of particulate organic matter in French forest soils, Geoderma, 342, 65–74, https://doi.org/10.1016/j.geoderma.2019.02.008, 2019.

Soucémarianadin, L. N., Cécillon, L., Guenet, B., Chenu, C., Baudin, F., Nicolas, M., Girardin, C., and Barré, P.: Environmental factors controlling soil organic carbon stability in French forest soils, Plant and Soil, 426, 267–286, https://doi.org/10.1007/s11104-018-3613-x, 2018.

Sparks, D. L.: Environmental Soil Chemistry, Second Edition., Academic Press, Burlington, 2003.

Sposito, G. and Sposito, G.: The Chemistry of Soils, Third Edition, Third Edition., Oxford University Press, Oxford, New York, 2016.

Stan Development Team: Stan User's Guide, 2024.

Stewart, C. E., Paustian, K., Conant, R. T., Plante, A. F., and Six, J.: Soil carbon saturation: Concept, evidence and evaluation, Biogeochemistry, 86, 19–31, https://doi.org/10.1007/s10533-007-9140-0, 2007.

Strickland, M. S., Osburn, E., Lauber, C., Fierer, N., and Bradford, M. A.: Litter quality is in the eye of the beholder: Initial decomposition rates as a function of inoculum characteristics, Functional Ecology, 23, 627–636, https://doi.org/10.1111/j.1365-2435.2008.01515.x, 2009.

Ulrich, E.: Le réseau RENECOFOR : Objectifs et réalisation, Revue forestière française, 47, 107–124, https://doi.org/10.4267/2042/26634, 1995.

Van Der Kellen, I., Derrien, D., Ghanbaja, J., and Turpault, M.-P.: Recent weathering promotes C storage inside large phyllosilicate particles in forest soil, Geochimica et Cosmochimica Acta, 318, 328–351, https://doi.org/10.1016/j.gca.2021.12.009, 2022.

https://doi.org/10.5194/egusphere-2026-6489
Preprint. Discussion started: 9 November 2026
© Author(s) 2026. CC BY 4.0 License.

Vávřová, P., Penttilä, T., and Laiho, R.: Decomposition of Scots pine fine woody debris in boreal conditions: Implications for estimating carbon pools and fluxes, Forest Ecology and Management, 257, 401–412, https://doi.org/10.1016/j.foreco.2008.09.017, 2009.

Vehtari, A., Gelman, A., and Gabry, J.: Practical Bayesian model evaluation using leave-one-out cross-validation and WAIC, Statistics and Computing, 27, 1413–1432, https://doi.org/10.1007/s11222-016-9696-4, 2017.

Viskari, T., Pusa, J., Fer, I., Repo, A., Vira, J., and Liski, J.: Calibrating the soil organic carbon model Yasso20 with multiple datasets, Geoscientific Model Development, 15, 1735–1752, https://doi.org/10.5194/gmd-15-1735-2022, 2022.

von Fromm, S. F., Hoyt, A. M., Lange, M., Acquah, G. E., Aynekulu, E., Berhe, A. A., Haefele, S. M., McGrath, S. P., Shepherd, K. D., Sila, A. M., Six, J., Towett, E. K., Trumbore, S. E., Vågen, T.-G., Weullow, E., Winowiecki, L. A., and Doetterl, S.: Continental-scale controls on soil organic carbon across sub-Saharan Africa, SOIL, 7, 305–332, https://doi.org/10.5194/soil-7-305-2021, 2021.

Wagai, R., Kajiura, M., and Asano, M.: Iron and aluminum association with microbially processed organic matter via meso-density aggregate formation across soils: Organo-metallic glue hypothesis, SOIL, 6, 597–627, https://doi.org/10.5194/soil-6-597-2020, 2020.

Wang, L., Zhou, Y., Chen, Y., Xu, Z., Zhang, J., Liu, Y., and Joly, F.-X.: Litter diversity accelerates labile carbon but slows recalcitrant carbon decomposition, Soil Biology and Biochemistry, 168, 108632, https://doi.org/10.1016/j.soilbio.2022.108632, 2022.

Wrightson, I., Anaraki, M. T., Fekete, I., Kotroczó, Z., Lajtha, K., and J. Simpson, M.: Ecological properties uniquely dictate molecular-level soil organic matter composition in a temperate forest in Central Europe with variation in litter deposition, Environmental Science: Processes & Impacts, 27, 763–778, https://doi.org/10.1039/D4EM00462K, 2025.

Yang, Y., Xie, H., Mao, Z., Bao, X., He, H., Zhang, X., and Liang, C.: Fungi determine increased soil organic carbon more than bacteria through their necromass inputs in conservation tillage croplands, Soil Biology and Biochemistry, 167, 108587, https://doi.org/10.1016/j.soilbio.2022.108587, 2022.

Yu, M., Wang, Y., Jiang, J., Wang, C., Zhou, G., and Yan, J.: Soil Organic Carbon Stabilization in the Three Subtropical Forests: Importance of Clay and Metal Oxides, Journal of Geophysical Research: Biogeosciences, 124, 2976–2990, https://doi.org/10.1029/2018JG004995, 2019.

Zanella, A., Berg, B., Ponge, J.-F., and Kemmers, R. H.: Humusica 1, article 2: Essential bases – Functional considerations, Applied Soil Ecology, 122, 22–41, https://doi.org/10.1016/j.apsoil.2017.07.010, 2018.

Zhang, W., Yuan, S., Hu, N., Lou, Y., and Wang, S.: Predicting soil fauna effect on plant litter decomposition by using boosted regression trees, Soil Biology and Biochemistry, 82, 81–86, https://doi.org/10.1016/j.soilbio.2014.12.016, 2015.